An-Najah National University

Faculty of Graduate Studies

Cellulose Based Film with Schiff Base Functionality : Preparation and Application in Adsorption of Toxic Metals form Wastewater

By:

Noor Raid Mahmoud Nairat

Supervisor

Prof. Othman Hamed

Co-Supervisor

Prof. Shehdeh Jodeh

This Thesis is Submitted in Partial Fulfillment of the Requirements for the Degree of Master of Chemistry, Faculty of Graduate Studies, at An-Najah National University, Nablus, Palestine.

2021

Cellulose Based Film with Schiff Base Functionality : Preperation and Application in Adsorption of Toxic Metals from Wastewater

By

Noor Raid Mahmoud Nairat

This thesis was successfully defended on 16/12/2021 and approved by:

Defense Committee Members	**Signature**
- Dr. Othman Hamed / Supervisor	.....
-Dr. Shehdeh Jodeh / Co-Supervisor	.....
- Dr. Abedalhadi deghles / External Examiner	.....
- Dr. Ibrahim Abu Shqair / Internal Examiner	.....

Dedication

To my lovely parents, my dear brothers, my lovely sister thank you for your continuous support, I hope from my Allah to protect you for me.

To my dear friends who still with me in all my steps of my life.

To every teacher who taught me in my life, Thanks for your support that reach me to what I am in it.

To everyone was in my life, also still, offer the support, and love for me.

Acknowledgment

Firstly, the biggest and greatest thanks to my Allah, who always guided me to the right way, and give me all wanted things to continue in the right way.

Big thanks to my family, my friends and every one gives support for me whether financial or moral support.

Special thanks to my research supervisors Dr. Othman Hamed and Dr. Shehdeh Jodeh to give me the opportunity to work with them. Special thanks to Dr. Othman for his Guidance and advices to obtain good research and good results. Special thanks for my friend, Dr. Ghadeer Hanbali.

In addition, I would like to thank the thesis committee members to give me some of their times to read my thesis and provide useful suggestions and advices.

Also, great and special thanks for Palestinian Water Authority and Middle East Desalination Research Center (MEDRC) MSc for their financial support for my project.

Finally, I would like to thank to Mr. Nafeth Dwekat, my supervisor in the chemistry lab, and all lab technicians at An-Najah National University, for their cooperation and patience on my requests during my research work.

الإقرار:

أنا الموقع أدناه مقدم الرسالة التي تحت عنوان

Cellulose Based Film with Schiff Base Functionality : Preparation and Application in Adsorption of Toxic Metals form Wastewater

أقر بأن ما اشتملت عليه هذه الرسالة إنما هي من نتاج جهدي الخاص، باستثناء ما تمت الاشارة اليه حيثما ورد، وأن هذه الرسالة ككل أو أي جزء منها لم يقدم من قبل لنيل أي درجة علمية أو بحث علمي أو بحثي لدى أي مؤسسة تعليمية أو بحثية أخرى

Declaration

The Work Provided In This Thesis, Unless Otherwise Referenced, Is My Research Own Work, And Has Not Been Submitted Elsewhere For Any Other Degree Or Qualification.

Student's name: اسم الطالبة:

Signature: التوقيع:

Date: التاريخ:

List of contents

NO.	subject	page
	Dedication	iii
	Acknowledgment	iv
	Declaration	v
	List of Contents	vi
	List of Tables	ix
	List of Figures	xi
	List of scheme	xii
	List of Abbreviations	xiii
	Abstract	xiv
	Chapter One: Introduction	1
1.1	Background	1
1.2	Cellulose	9
1.2.1	Chemically modified cellulose for removing heavy metals	12
1.2.2	Cellulose as a metal adsorbent	16
1.3	Aniline	17
1.4	Glycine	19
1.5	Scope of the study	20
	Chapter Two: Experimental	22
2.1	Material	22
2.2	Instrumentation	22
2.3	Methods	23
2.4	Polymers preparation	24
2.4.1	Preparation of cellulose acetoacetate (Cell-AA)	24
2.4.2	Preparation of cellulose β-aminoester using aniline (Cell-β-AN)	25
2.4.3	Preparation of cellulose β-aminoester using glycine (Cell-β-GL)	26

2.4.4	Polymer solubility in water	26
2.5	Purification of contaminated water from lead metal using cellulose polymer	26
2.5.1	Preparation of lead solutions	26
2.5.2	Calibration curve	27
2.5.3	Batch adsorption experiments	28
2.6	Wastewater purification	38
	Chapter Three: Results And Disscusion	39
3.1	Synthesis of cellulose-acetoacetate polymers	39
3.1.1	FT-IR of cellulose and cellulose acetoacetate	42
3.1.2	TGA analysis and thermal stability	44
3.2	Synthesis of cellulose β-aminoester using aniline	45
3.2.1	FT-IR of cellulose β-anilinoacetonate	47
3.2.2	TGA analysis and thermal stability of cell-β-AN	49
3.3	Synthesis of cellulose β-glycineacetoester (Cell-β-GL	49
3.3.1	FT-IR of cellulose β-glycineacetonate	52
3.3.2	TGA analysis and thermal stability of Cell-β-GL	53
3.4	Toxic metal ions extraction	54
3.4.1	Optimum adsorption conditions	55
3.5	Wastewater purification from metals	61
3.6	Polymer adsorption cycle	63
3.7	Adsorption analysis	63
3.8	Adsorption kinetics of pb^{+2} ions on cellulose based polymers	66
3.9	Thermodynamics study	72
	Conclusion	75
	Recommendation of future work	76
	References	77
	الملخص	ب

List of Tables

NO.	Subject	Page
2.1	Effect of polymer dose on the lead removal efficiency for polymer Cell-AA.	29
2.2	Effect of polymer dose on the lead removal efficiency for polymer Cell-β-AN .	29
2.3	Effect of polymer dose on the lead removal efficiency for polymer Cell-β-GL .	29
2.4	Effect of contact time on the lead (Pb^{2+}) removal efficiency for polymer Cell-AA	30
2.5	Effect of contact time on the lead (Pb^{2+}) removal efficiency for polymer Cell-β-AN	31
2.6	Effect of contact time on the lead (Pb^{2+}) removal efficiency for polymer Cell-β-GL	31
2.7	Effect of temperature on the lead removal efficiency for polymer Cell-AA.	32
2.8	Effect of temperature on the lead removal efficiency for polymer Cell-β-AN .	32
2.9	Effect of temperature on the lead removal efficiency for polymer Cell-β-GL .	33
2.10	Lead nitrate concentration effect on lead removal efficiency for polymer Cell-AA.	34
2.11	Lead nitrate concentration effect on lead removal efficiency for polymer Cell-β-AN .	34
2.12	Lead nitrate concentration effect on lead removal efficiency for polymer Cell-β-GL.	34
2.13	Effect of pH on the lead removal efficiency for polymer Cell-AA.	35
2.14	Effect of pH on the lead removal efficiency for polymer Cell-β-AN .	36
2.15	Effect of pH on the lead removal efficiency for polymer Cell-β-GL.	36
2.16	Recycling of polymer Cell-AA	37
2.17	Recycling for polymer Cell-β-AN	37

2.18	Recycling for polymer Cell-β-GL.	38
3.1	The adsorption results for Pb(II) ions using the three polymers.	61
3.2	Results of the center of analyzes for the Concentration of toxic metals using Cell-AA polymer.	62
3.3	Results of the center of analyzes for the Concentration of toxic metals using Cell-β-AN polymer.	62
3.4	Results of the center of analyzes for the Concentration of toxic metals using Cell-β-GL polymer.	66
3.5	Langmiur and Freundlich parameters for the adsorption of Pb^{+2} ions by cellulose based polymers	71

List of Figures

NO.	Subject	Page
1.1	Molecular structure of cellulose polymer showing the anhydroglucose monomer in the chair conformation and the glycosidic link	9
1.2	Intramolecular and intermolecular hydrogen bonding in cellulose polymer	10
1.3	Structure of modified cellulose	13
1.4	Structure of CMC.	14
1.5	Structure of cell-p-PDA polymer	15
1.6	Structure of cellulose amine polymer	16
1.7	Structure of aniline	17
1.8	Resonance structures of aniline	18
1.9	Structural formula of glycine	19
2.1	Calibration curve of lead Pb(II)	27
3.1	A representative figure the interaction between cellulose and LiCl/DMAc	40
3.2	Mechanism of transesterification of NCC	42
3.3	FT-IR spectrum for cellulose	43
3.4	FT-IR spectrum for Cell-AA	44
3.5	TGA and DTG analysis for cell-AA polymer.	45
3.6	Preparation of cellulose β-anilinoacetonate (Cell-β-AN) using aniline.	46
3.7	Reaction mechanism for the synthesis of cellulose β-anilinoacetonate.	46
3.8	The FT-IR spectrum of aniline.	47
3.9	FT-IR spectrum for Cell-β-AN.	48
3.10	TGA and DTG analysis for Cell-β-AN	49
3.11	Preparation of cellulose β-aminoacetonate	50
3.12	Mechanism of synthesis of cellulose β-glycineacetonate	51
3.13	Cellulose aminoacetonate as a multidentate chelating agent (Shiff base)	52

3.14	FT-IR spectrum for Cell-β-GL	53
3.15	TGA and DTG analysis for Cell-β-GL polymer	53
3.16	The effect of the three polymers dose on the removal efficiency.	56
3.17	The effect of contact time on the removal efficiency for the three polymers.	57
3.18	The effect of temperature on the removal efficiency for the three polymers	58
3.19	The effect of lead solution concentration on the removal efficiency for the three polymers.	59
3.20	The effect of pH on the removal efficiency for the three polymers.	60
3.21	Regeneration and adsorption efficiency for the three polymers	63
3.22	A) Langmiur adsorption model and B) Freundlich adsorption model of Pb^{+2} ions on cellulose based polymers	65
3.23	**A**) Pseudo first-order model for the adsorption of Pb^{2+}, **B**) Pseudo-second order model for the adsorption of Pb^{2+} ions onto Cell-AA, Cell-β-AN, and Cell-β-GL. **C)** Intra-particle diffusion model for the adsorption of Pb^{2+} ions onto Cell-AA, Cell-β-AN, and Cell-β-GL at various concentrations.	68
3.24	Adsorption thermodynamics of Pb^{+2} ions onto Cell-AA, Cell-β-AN and Cell-β-GL.	72
3.25	Liquid film diffusion model plots for the adsorption of Cell-AA, Cell-β-AN and Cell-β-GL.	74

List of Scheme

No.	Scheme	Page
3.1	Preparation of cellulose acetoacetate from cellulose.	41

List of Abbreviations

Symbol	Abbreviation
WHO	World Health Organization.
EPA	Environmental Protection Agency
CNC	Cellulose Nanocrystalline
BOD	Biological Oxygen
COD	Chemical Oxygen
CMC	Chemically Modified Cellulose
Cell-p-PDA	Cellulose diamine
OISW	Olive Industry Solid Waste
MNCs	Magnetic Cellulose Nanocrystalline
DMAc	Dimethyl acetamide anhydrous
LiCl	Lithium chloride
t-BAA	tert-butyl acetoacetate
TGA	Thermogravimetric analyser
FAAs	Flame Atomic Absorption Spectrometer
FT-IR	Fourier transform infrared
DSC	Differential Scanning Calorimetry
Cell-AA	Cellulose -acetoacetate
Cell-β-AN	cellulose β-aminoester using aniline
Cell-β-GL	cellulose β-aminoester using glycine

Cellulose Based Film With Schiff Base Functionality : Preparation And Application In Adsorption Of Toxic Metals Form Wastewater

By:
Noor Raid Mahmoud Nairat
Supervisor
Prof. Othman Hamed
Co-Supervisor
Prof. Shehdeh Jodeh

Abstract

The main objective of this work is to use the olive industry waste material as a base for making polymers suitable for wastewater purification from toxic heavy metals. Cellulose extracted from the olive industry solid waste was used as a starting material for the preparation of three cellulose derivatives with several coordination sites for metal ions and useful adsorbents for metal ions from sewage. The cellulose polymers contain the pendants groups acetylacetonate, amine acetonate and amino acid acetonate. They were prepared in a three step process that include dissolution of cellulose in 8 wt% LiCl/DMAc, reacting the cellulose with t-butyl acetoacetonate, then with either the amino acid glycine or aniline. The polymer structures were determined by FT-IR. The thermal stabilities of the polymer were also investigated, they should stability a temperature of about 200 ^{o}C. The adsorption efficiency of the three cellulose-based polymers toward Pb(II) from an aqueous solution was investigated as a function of adsorbent dose, metal ion concentration temperature, pH, and time. The adsorption parameters that give the highest adsorption efficiency were determined. The highest efficiency of the Cell-AA and Cell-β-GL

polymers for lead ion were 94.9% and 91.6%, respectively, obtained at concentration of 10 ppm, 50 mg of each polymer, at 30 °C and 9 pH upon shaking for a period of 120 minutes. For the Cell-β-AN polymer, the highest efficiency toward lead ion was 86.7% at approximately the same previous parameters. In addition, the cellulose-based polymers showed an excellent efficiency toward most of metal ions present in the sewage sample. The highest adsorption efficiency was at pH of about 9, 30 ^{o}C and with 50 mg of polymer dose. The high adsorption efficiency of the cellulose-based polymers could be attributed to the presence of various coordination sites which includes hydroxyl, amino, carbonyl and aryl group.

Chapter One

Introduction

1.1 Background

Water is an extremely important substance in all part of the environment. About 97.6% of Planet's water is found in the oceans and seas. Another fraction distributed in the following ratio (ice and snow in snowpacks, polar ice cap and glaciers 2.05%, underground 0.4%, vapor in atmosphere 0.0013%). Surface water is found in streams, lakes and reservoir which form 0.0092%. The water present in ocean and seas is salt water and not suitable for drinking, while the remaining 3% is fresh water which comes from few sources such as rivers, lakes, streams, and underground water. Although water cover 72% of earth's surface, the proportion of drinkable water doesn't exceed 0.3% of the World's water stock. Until now, water resources are still suffering from pollution. Around the world, water pollution causes death and diseases, about 1400 people die every day due to water pollution [1-5]. According to the World Health Organization (WHO) report, by 2050, half of the world's population will live in areas suffering from water worry [6].

Globally, problems with the quantity and quality of water supply still exist and become more serious in some respects. These problems include increased water consumption due to population growth, pollution of drinking water by improperly discarded hazardous wastes [1]

Water pollution become a critical global problem and major health issue for living organism and ecosystem, because of growth, increasing industrialization, energy generation and human causes. [7-9]

Many technologies that are easy to use are developed as a part of the continual efforts to form water free from contamination, good quality, sustainable and economically feasible [10]

Since World War II there has been an incredible growth within the manufacture and use of synthetic chemicals industrial activities. Industrial waste, agricultural waste, sewage water and the increase load of population have contaminated the water with many toxic substances such as toxic heavy metals, organic material, dyes and other. [11,12]

The threshold limit of toxicity is defined as the average concentration of toxic material or metal that normal person may be exposed for 7-8 hours per week for lifetime without harm [13]. If concentration of toxic heavy metal in water exceeds the threshold limit, then it is considered pollutant and causes harmful effect to the creature [14]. Each toxic metal has its threshold limit value according to its toxicity.

Heavy metal found in nature are the elements having specific density more than 5 g/cm^3 (five time the density of water) and atomic weight higher than 40 [15]. Among the toxic heavy metals that pose a risk are lead (Pb), cadmium (Cd), mercury (Hg), chromium (Cr), Nickel (Ni), Zinc (Zn), Copper (Cu), Cadmium (Cd) and arsenic (As) [16,17]. They mainly come

from medical, agricultural, plumbing, household chemicals, body care products, textiles, tanneries, plastics, and industrial activities.

Some heavy metals are important for life and are called essential element which are required for a variety of physiological and biochemical functions. However, they will be toxic when present in large concentration [18,19].

Heavy metals may enter a human body in four ways from; ingestion of contaminated food, drinking contaminated water, inhalation from the atmosphere, and by skin contact with it. When heavy metals are swallowed or inhaled into our bodies pose a threat because heavy metals are highly soluble in water, they are nonbiodegradable and tend to accumulate in food chains, and are nonbiodegradable. Metalloids tend to form covalent bonds with organic groups, making them show extreme toxic properties. For example, lead and mercury can bind to sulphydryl groups of the protein [20]. Organisms hide the active detoxify metal ions within a protein or depositing them in intracellular granules in an insoluble form for long-term storage, they bioaccumulate in our system.

Bioaccumulation can be defined as; the rise in concentration of toxic chemicals in biological organisms over time [21,22]. This bioaccumulation causes toxic biological and physiological complications. So, when these heavy metals consumed by the humans through drinking water, they produce serious health issues like cancers, nervous system diseases, organ damage, and death in rare instances [23].

Toxicity of heavy metal depend on several factors, such as the organism which expose to it, type of metal, its biological rule, its nature, the period at which the organisms are exposed to metal. If one organism is affected, this means that all food chain will be affected. Since humans are usually the last of the food chain [20].

Two types of damage may be result when organism is exposed to heavy metal, “direct” and “indirect” damage. In the indirect damage, the reactive oxygen and nitrogen species are produced, which can cause oxidative stress, which can lead to a variety of diseases. On the other hand, the heavy metal causes “direct” damage which is the result of conformational changes occur to the biomolecules [24].

Carcinogenic metal ions produce redox reactions in biological systems which generate free radicals that cause oxidative damage to proteins and DNA, consequently leading to cell cycle modulation, apoptosis or carcinogenesis. The accumulation of heavy metal such as As, Hg, Cd and Ni will destroy the main metabolic process of human body since they have strong affinity for sulfur, when they bond via thiol group (-SH), hinder the functioning of enzyme [15,25].

Chronic level ingestion of toxic metals causes harmful impact and become perceptible after several years of exposure. Cadmium causes cardiac failure cancers, cerebrovascular infarction, lung cancer, emphysema and osteoporosis [26]. Zinc may cause icterus, prostate cancer, liver failure, kidney failure and anemia [27]. Copper causes widespread capillary

damage, hepatic and renal damage, depression, and central nervous system irritation [28]. Mercury causes mutagenic, mental retardation, neurological and renal damage [29]. Arsenic causes melanosis nausea, skin cancer, nerve inflammation and muscle weakness [30]. Also, lead heads the threats even at extremely low concentration. It can exist in divalent form. lead poisoning can cause lung and liver damage, loss of appetite, gastrointestinal tract and urinary damage, fetal brain damaging, anemia, anorexia, vomiting, nervous and circulatory system deterioration. It usually reaches water from corrosion of water pipes used in distribution system, batteries manufacturing, auto exhaust (from gasoline), paints and pigment, mining activities, industrial wastewater, bronze product, ceramic and glass industries, dust, and soil containing lead that comes from fertilizer and pesticide. Therefore, removal of these metals from water became necessary [31,32].

The maximum contaminants levels that protect human health are called the Primary Drinking Water Standards. The Primary Drinking Water Standards for lead equal 15 ppb. According to the Environmental Protection Agency (EPA) and the WHO, maximum allowable concentration of lead in drinking water are 10 ppb and 15 ppb respectively [33-36].

The three major goals in water pollution are detecting pollutant, treating them and limiting their discharge into the aquatic environment.

Recycling of wastewater released from industrial and human activities become very necessary. Several methods are used for purifying wastewater

from toxic heavy metals before it discharges into waterway or reaches the domestic usage. Among the most effective technologies are precipitation, membrane filtration, electrodialysis, electrochemical treatment, coagulation [37], flotation [38], cementation [39], solvent-solvent extraction [40], ion exchange [41], chemical oxidation [42], reverse osmosis [43], use of electromagnetic radiation [44] and adsorption [45].

Each of the above-mentioned methods has its own advantages and constraints. Most of methods are less efficient, consume high energy, provide poor removal efficiency, generate hazardous waste sludge, require high labor, and not economically feasible [46].

Compared with other techniques, the adsorption method received the highest attention due to its simplicity, availability, profitability, practicality, inexpensiveness, cleanliness, eco-friendliness, adsorbent reusability, energy saving, less sludge production, easy to handle, have high efficiency and selectivity [47,48].

Adsorptions occur when adsorbate moves out from the liquid phase (contaminated solution) and adheres to the surface of an adsorbent through physical or chemical interaction. In adsorption science, the solid surface on which the adsorption process takes place is called adsorbent, and the substance that is adsorbed on the solid surface is called as adsorbate [49].

The adsorbent is expected to carry the following properties [50]:

1) High selectivity to achieve sharp separation when components are present in certain types of mixtures.

2) High adsorbent capacity which strongly depends on surface area, surface group and porosity. As adsorbent capacity increases, small amount of adsorbent required.
3) Kinetically favorable to obtain fast adsorption rate
4) Good mechanical strength and hardness to resist corrosion, struggle cracks and increase its life
5) Thermally stable to be stable at high temperature.
6) Chemically stable to resist changes in its composition due to chemical reactions that may happened such as oxidation.
7) Can be recycled to be commercially usable.

Activated carbon is one of the adsorbents that have been used to remove metals form wastewater, but the high material processing costs made it less attractive and hence its use is limited [51]. It's necessary to develop readily available and low-cost adsorbents for adsorption of heavy metals from wastewater.

Industrial waste and natural based materials such as clay [52], zeolites [53, 54] and peats [55-56] were also evaluated as adsorbents for toxic metals. Industrial waste included metal hydroxide [57], sludge, red mud, and fly ash [58].

Therefore, renewable, low-cost adsorbents derived from agricultural waste materials have been considered attractive alternatives for water purification [59]. Among the natural based adsorbents cellulose [60], lignin, chitosan, and hemicellulose were the most attractive. Their adsorption capacity is

lower than activated carbon because it has a higher surface area, but they can be generated relatively at a lower cost . They are economically feasible, environmentally friendly, and highly efficient for removal of heavy metal ions from wastewater [61]

Cellulosic based adsorbents obtained from waste materials such as Kenaf [62,63], cotton linters [64], wheat straw [65], wood sawdust [66], rice husk [67] were prepared and investigated for the adsorption of several metals such as Cd^{2+}, Cu^{2+}, Mn^{2+}, Mg^{2+}, Sr^{2+}, Al^{3+}, Co^{2+}, Ni^{2+}, Cr^{3+}, $Zn^{2+}$and Pb^{2+}ions. Many of agricultural wastes contain a large functional group like aldehyde, amine, and keto group, etc. These qualities increase the efficiency of agricultural waste for removal of toxic pollutants and provide them with an impressive adsorption capacity.

Recently, a breakthrough was made in nanotechnology as a promising technique for metal removal from wastewater [68,69]. Nanoparticles possess a higher specific surface area than bulk particles and can be functionalized with various chemical groups, which increase their affinity toward contaminants. Also have nanosized pores which assist in the sorption of contaminants. These two important properties make them very effective as sorbents. Moreover, nanosorbents can be reused via removing the adsorbed pollutants, that way regenerating them.

Nanoparticle from natural materials were the most promising, the rapid progress made in the nanoscience, especially with cellulose nanocrystalline (CNC), offers a potential new material for use in wastewater treatment.

CNC is unique regarding its functional groups, high surface area combined with a rigidity, which may result in improved purification efficiency. Also, many cellulose derivatives were prepared and used for waste-water purification. Despite all the rapid progress in the nanocellulose adsorbents still many Cellulose based materials and derivatives have not been explored in wastewater purification [70].

In this work, new cellulose based adsorbent was prepared from reacting oxidized cellulose with the amino compounds aniline and glycine. Both convert oxidized cellulose to Schiff base with high affinity for metals.

1.2 Cellulose

Cellulose is the most renewable and abundant biopolymer in earth. This organic polymer have a formula $(C_6H_{10}O_5)_n$. The molecular structure of cellulose is a homopolysaccharide consisting of a linear chain of many thousands of β-D-anhydroglucopyranose monomer coupled with β-1,4-glycosidic links. The six-membered heterocyclic β-D-anhydroglucopyranose is usually found in a chair conformation [71].

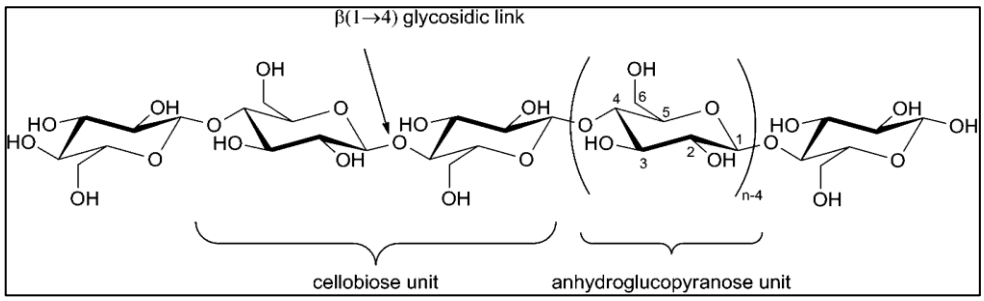

Fig (1.1): Molecular structure of cellulose polymer showing the anhydroglucose monomer in the chair conformation and the glycosidic link

Cellulose have large number of hydroxyl group, which can be divided into three groups: C-6 primary OH and C-2 and C-3 are secondary OH. These multiple hydroxyl groups form hydrogen bonds with oxygen atoms on a neighbor (inter molecular hydrogen bonding) or on the same chain (intra molecular hydrogen bonding), making the chain contact together and forming high tensile strength microfibrils. Hydroxyl groups have affinity to heavy metal ions [50].

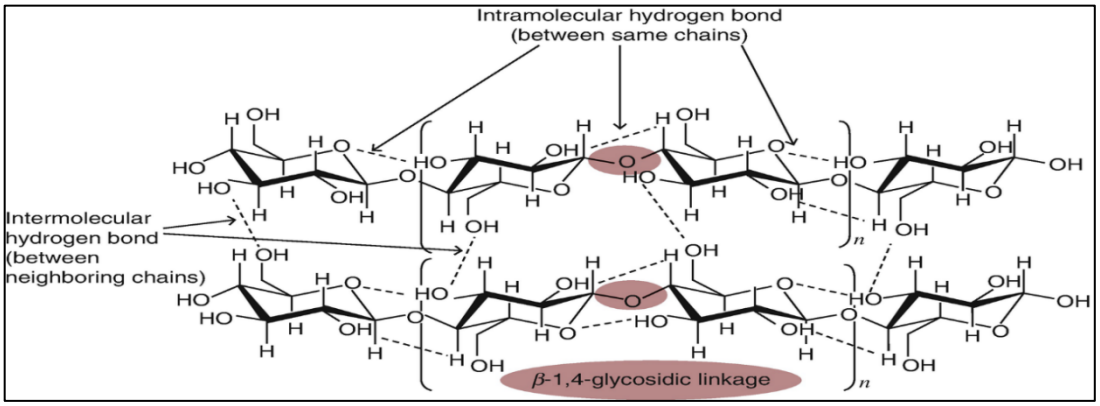

Fig (1.2): Intramolecular and intermolecular hydrogen bonding in cellulose polymer

Cellulose has a molar mass of 162.1406 g/mol per glucose unit, it has a density of 1.5 g/cm^3, it decomposes at melting point 260-270 ºC, it is biodegradable, also it is insoluble in water and most organic solvents because it has hydrophilic regions [72].

Cellulose is found in nature in several marine animals, fungi, bacteria invertebrates, amoeba, plants, algae, and mineral. However, plant fiber is the main source of cellulose. Cellulose is found in the structural component of cell walls in most organisms. Some bacteria also excrete bacterial cellulose to form porous biofilms. Annually, 10^{11}-10^{12} tons of cellulose are

synthesized in a relatively pure form. 90% of cotton fiber content is cellulose, and a dried hump has about 57% of cellulose [71].

In cellulose chemical formula $(C_6H_{10}O_5)_n$, n is the degree of polymerization (DP), which represents the number of repeated monomers. Many cellulose properties depend on degree of polymerization (chain length). Wood cellulose has DP of about 10000 glucopyranose unit and 15000 unit in plant cell [73]. Melting temperature and mechanical strength increase with increasing DP.

Cellulose fibrils are composed of crystalline and amorphous regions. Cellulose characteristics are affected by the cellulose crystalline structure. For example, as the proportion of crystalline increases, the flexibility of cellulose's amorphous decreases due to the strong and tightly packed hydrogen bonding network. The hydrogen bonding networks have a wide orientation, resulting in different allomorphs of cellulose. Chemical oxidation or enzymatic treatment to cellulose fibrils produce flexible cellulose nanofibrils. If amorphous fibril regions hydrolyze with a strong acid, short rigid cellulose nanocrystal will produce (few nm in length). This material has many desirable properties [74].

Cellulose has many properties make it a good choice as a metal adsorbent: naturally available, nontoxic, thermally and chemically stable, biodegradable, have high tensile and compressive strength. Cellulose polymer has a large and linear chain, this chain contains a large number of hydroxyl group which stick out from it and form intermolecular hydrogen

bond, this bond strengthens interaction between neighboring cellulose molecules [75]. Many cellulose derivatives can be produced if the hydroxyl groups are modified and used for an unlimited number of applications [76].

In this research, cellulose was prepared at An-Najah National University in Palestine from the solid waste of the olive industry by subjecting it to kraft pulping and then bleaching it using a multi-step process. There is a huge amount of unused olive mill waste produced every year all over the world which poses a severe environmental problem. Olive mills produce two types of waste, solid waste (jeft) and liquid waste (zebar), which contain toxic levels of polyphenols, as well as require high level of biological oxygen (BOD) and chemical oxygen (COD). Disposing of this waste is a worrying environmental problem. The common way to get rid of this waste is to spread solid waste on the soil and expose it to the sun to dry and use it for heating, which produce carbon dioxide gas that rise to the atmosphere and increase global warming, while the liquid oil is disposed of through the sewage network. The challenge is to turn these wastes into useful and low-cost material [77,78]

1.2.1 Chemically modified cellulose for removing heavy metals

Chemical modification of cellulose decreases the crystalline structure, destroys the hydrogen bonds and makes more efficient binding sites (more reactive OH groups) to attack with other functional groups and give better adsorption [50].

There are two primary methods used for cellulose modification:

1) Chemical bonding of OH and NH_2 groups to produce cross linking network (gel) which is insoluble in water.
2) Control of polysaccharide movement on surface to produce hybrid materials by grafting response. [76]

Various chemically modified cellulose polymers were prepared and used in water purification. A different proportion of sodium hypochlorite (NaOCl) and octenyl succinic anhydride (OSA) were used to modify cellulose powder. This modification added carbonyl functional group with good affinity for adsorption of Cu(II) heavy metal (fig 1.2). The simultaneous esterification and oxidation accelerate metal absorption process because higher degree of carbonyl groups substitution in the cellulose. This chemically modified cellulose (CN_1O) adsorbed about 85% of Cu(II) ion in 15 min under natural pH at room temperature. [79]

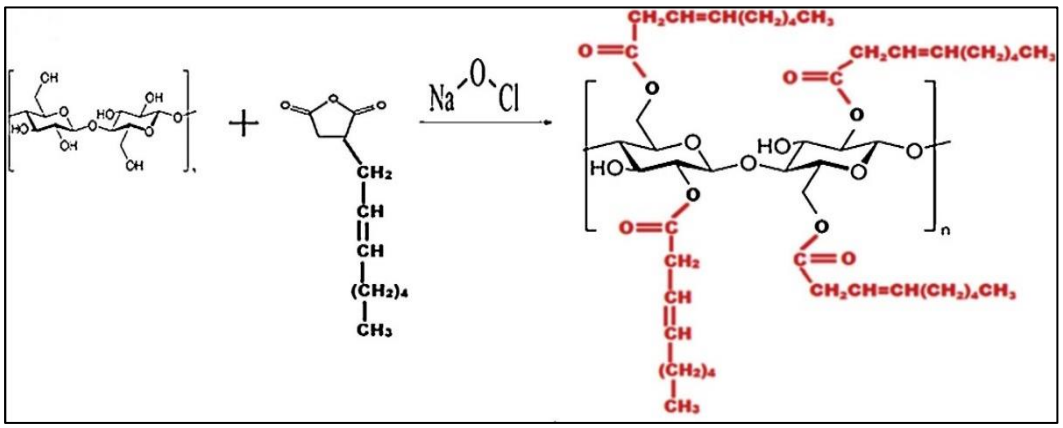

Fig(1.3): structure of modified cellulose

In another research chemically modified cellulose (CMC) was prepared by grafted cellulose with the vinyl monomer glycidyl methacrylate using ceric ammonium nitrate and was functionalized by addition of thiosemicarbazide

which containing C=S and amino groups then used to adsorb heavy metal (Fig 3). The final product was used in removal of Hg(II), Cd(II) and acid fuchsin. The adsorption was described by pseudo second order kinetic model. Langmuir adsorption isotherm models was applied to describe isotherm constant [80].

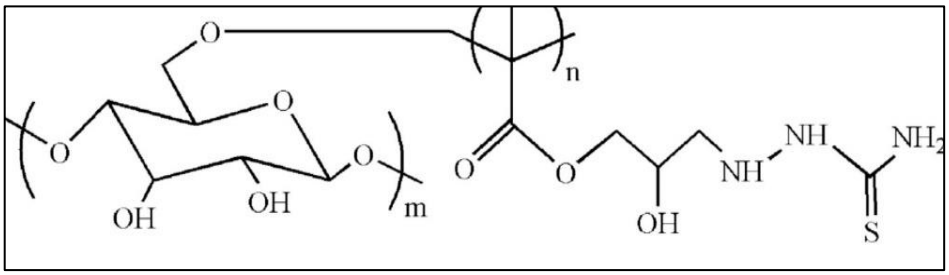

Fig(1.4): Structure of CMC

Novel adsorbent based on cellulose was designed by cross-linking NCC chain with 1,4-phenyldiamine, and then reduced by $NaBH_4$ to the final cellulose diamine (cell-p-PDA) product as shown in fig 1.5. The NCC used in this work was extracted from olive industry solid waste (OISW). The final product was used in removal of $Cu^{2+}$and Pb^{2+}. The prepared cell-p-PDA was showed an excellent adsorption efficiency toward for most of the toxic metals present in sewage sample. The presence of various functional groups on polymer surface such as amino, hydroxyl, and aryl also the semi-crown ether structure plays a key role in the cell-p-PDA polymer high extraction efficiency. The overall kinetic in each case is best described by the pseudo-second order approach [81].

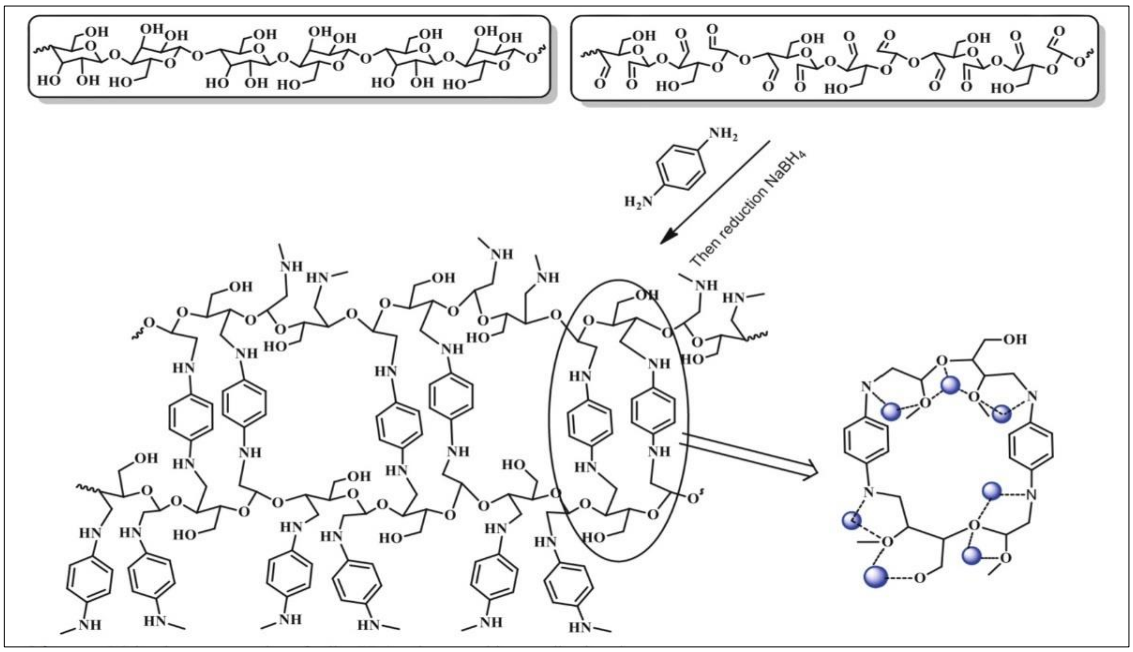

Fig (1.5): Structure of cell-p-PDA polymer

The three steps method were developed to synthesis a novel cellulose amine polymer from cellulose and 1,2-phenylenediamine as a bidentate chelating agent. This process involves oxidation of cellulose to aldehyde, then conversion the oxidized cellulose to imine which is reduces to amine by sodium borohydride. This cellulose derivative contains multiple coordination site as shown in fig 6. The presence of hydroxyl, ether, aromatic and amine functional groups in cellulose amine polymer made it a novel adsorbent for Fe(III), Pb(II) and the other toxic metal ions in sewage sample. A multistep pulping and bleaching process was applied to extract cellulose powder from OISW. The adsorption efficiency of the cellulose amine polymer toward Fe(III), Pb(II) was investigated as a function of adsorbent dose, temperature, pH and time. Kinetic study result that the adsorption isotherm follows a Langmuir isotherm model [82].

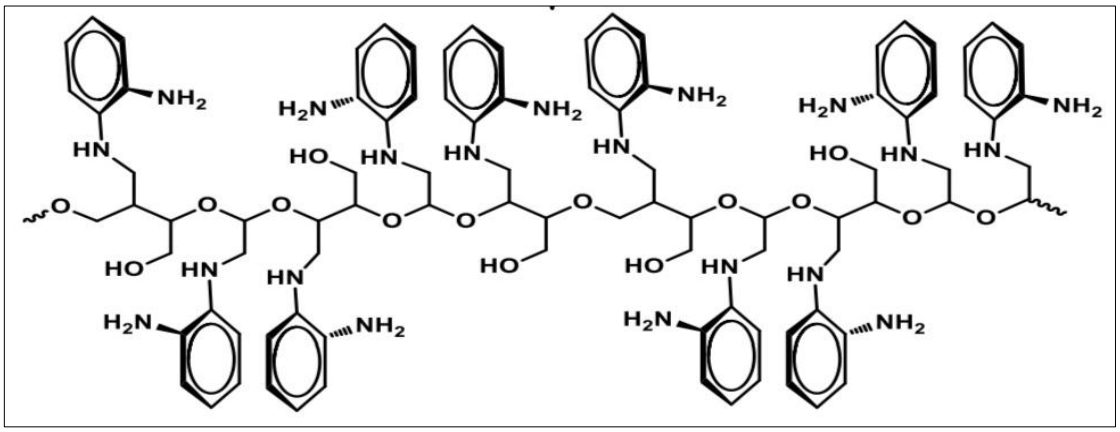

Fig (1.6): Structure of cellulose amine polymer

In other research, magnetic cellulose nanocrystalline (MNCs) was synthesised from cellulose powder and used as selective magnetic adsorbents for extraction of methylene blue from water. The cellulose powder used in this work was extracted from OISW. The extracted cellulose was converted to NCs by acid hydrolysis. Colloidal suspension method was applied to NCs to produce MNCs by treating it with a solution of $FeSO_4$, $FeCl_3.6H_2O$, and H_2O. The MNCs act as effective, economic and rapid adsorbent for inorganic nanoparticles from aqueous solutions. The thermodynamic studies revealed that the adsorption process is a spontaneous at various temperatures [60].

1.2.2 Cellulose as a metal adsorbent

Globally, the quantity of produced wastewater and its overall pollution load are increasing, due to economic development, population growth and accelerated urbanization. There is a necessity to purify the wastewater, and remove heavy metals mainly, we focused in this work to develop a new economic method to remove heavy metals using cellulose based material as adsorbents.

There are several well-known methods used to purify water from heavy metals, but these methods have some limitations. Adsorption was the simplest, renewable, and most efficient method used to purify wastewater. So, the efforts became direct towards using low-cost adsorbents.

Cellulose is a natural, renewable, biodegradable, non-meltable polymer and insoluble in most solvents due to crystallinity and hydrogen bonding. Cellulose can be modified chemically easily to be a good metal adsorbent. Because cellulose itself have lower adsorption capacity to remove heavy metals.

1.3 Aniline

Aniline is an aromatic amine with the formula ($C_6H_5NH_2$) and its structural formula shown in figure 7. Its IUPAC name is benzamine. Aniline is a light brown oily liquid having a musty odor. It's a flammable liquid, moderately soluble in water, soluble in most of aromatic molecule, boiling at about 184 ^oC, have 1.02 g/cm^3 density and 93.13 g/mol molecular weight, tend to darken when expose to air due to formation of strongly colored and oxidized impurities [83].

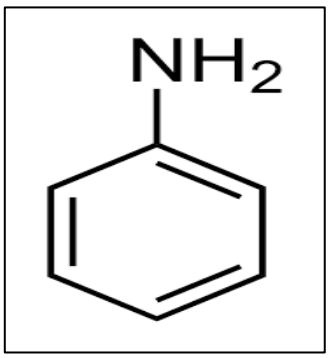

Fig (1.7): Structure of aniline

Aniline is toxic compound when it absorbed by skin or inhaled through the air, it irritated eyes, skin, and respiratory tract. Aniline reduced oxygen transport to tissue which cases methemoglobinemia, also causes hemolytic anaemia, because its destruct red blood cell [84].

Aniline is a weak base because nitrogen lone pair in unhybridized p orbital in NH_2 is conjugated with benzene ring π-electrons so it is not available for donation. Also due to resonance effect (fig 8) and inductive effect from the electronegative sp^2 carbon atom, this reduces the electron density around N-atom [85].

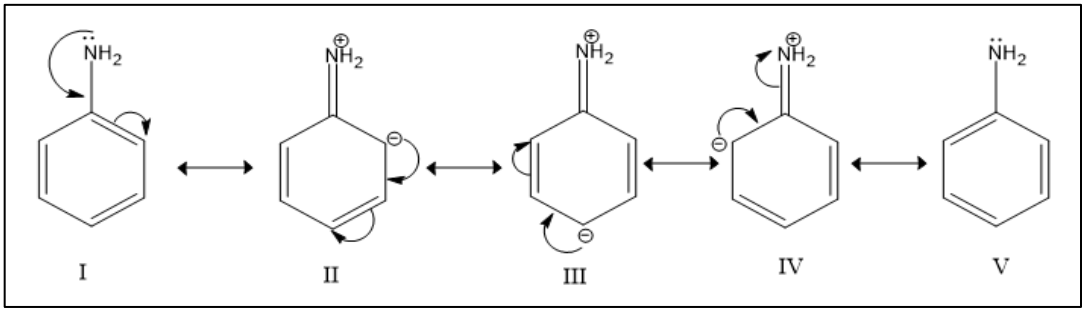

Fig (1.8): Resonance structures of aniline

Aniline is produced by catalytic reduction of nitrobenzene. A small amount of cyclohexylamine is produced as side product. There is another method involving amination of phenol [85]. The main uses of aniline are the manufacture of polyurethane, plastics, drugs, dyes, photographic, explosive, antioxidants and rubber chemicals. Apples, corn, rhubarb, beans, grains, rapeseed cake, and volatile component of black tea contain a small amount of aniline [86].

1.4 Glycine

Glycine or 2-Aminoethanoic acid is a proteinogenic amino acid, with the formula $C_2H_5NO_2$ and its structural formula shown in figure 9. It is a white crystalline solid with no odor, it can fit with hydrophilic or hydrophobic environments, it has a molar mass of 75.067 g/mol, and a density of 1.1607 g/cm^3. It melts at point of 233 ^oC [87].

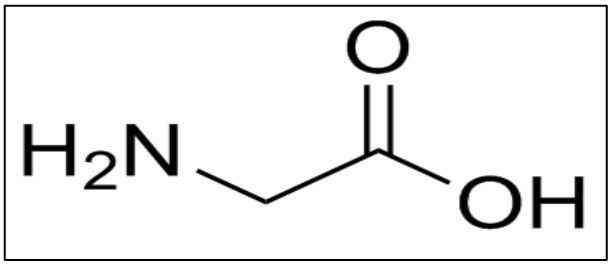

Fig (1.9): Structural formula of glycine

Glycine essential for many different muscle, cognitive and metabolic function. Its support muscular, digestive, immune, and nervous system. Glycine breaks down and transport nutrients like glycogen to use it by cell for energy. Glycine plays a vital rule in metabolism and nutrition of many organisms and play a supplementary rule in prevention of many diseases including cancer. The body can make glycine by itself, but it also consumed in the diet [88].

The primary sources of glycine are dairy, meat, legumes and fish. Glycine uses in animal and human food, also to synthesis a variety of chemical product and herbicides moreover used as an intermedia in the medicine such as thiamphenicol [89]. The two main process for glycine

manufactured is the Strecker amino acid synthesis, and amination of chloroacetic acid with ammonia [90,91].

1.5 Scope of the study

In this work, a novel adsorbent for waste water purification was prepared. The new adsorbent will be prepared by functionalization of microcrystalline cellulose with β-ketoester by dissolving it with Dimethylacetamide anhydrous (DMAc)/ lithium chloride anhydrous (LiCl) solution, then reacting it with tert-butyl acetoacetate (t-BAA) at 120 ºC, after that convert the ketone part to a Schiff base by reacting it with various amine (aliphatic and aromatic). Cellulose used in this work will be extracted from OISW [77,78] then hydrolyzed to microcrystalline. The target adsorbents are cellulose with β-aminoester attached to its backbone. The adsorbents are expected to have high affinity for various heavy metals since the functional groups are considered multidentate chelating agents. This property makes the target cellulose excellent candidate for application in waste water purification from both metals and organic materials.

The specific objectives of this thesis are to:

1. Design and synthesize of a cellulose based film with β-aminoester functionality.
2. Use it as an adsorbent for toxic metal ions such as lead(II) and others form wastewater.

The sub objectives of this thesis are to:

1. Synthesize of cellulose acetoacetate from cellulose extracted from olive oil industry solid waste.
2. Convert the cellulose acetoacetate to cellulose with β-aminoacetate functionality.
3. Develop a method to produce a film form cellulose β-aminoacetate.
4. Characterize the film and components by various spectroscopic techniques.
5. Evaluate the possibility of using the prepared film in adsorption of lead(II) from waste water.
6. Evaluate the effect of various parameters such as pH, adsorbent dose, adsorbate concentration, temperature, pH and time of adsorption efficiency.
7. Develop a process for regenerating the film and reuse.

Chapter Two

Experimental

2.1 Materials

All chemicals and reagents used in this work were purchased form Sigma-Aldrich chemical company (Jerusalem) and used as received. The chemicals include tert-Butyl acetoacetate (t-BAA), lithium chloride anhydrous (LiCl), N,N-dimethylacetamide anhydrous (DMAc), aniline, glycine, lead(II) nitrate, acetic acid, methanol and nitrogen gas (purity 99.9%). All reagents used were of analytical grade. Deionized water was used to prepare all solutions. Cellulose used in this work was extracted from olive industry solid waste (jeft) by a chemical process that was developed at the laboratories of An-Najah National University-Nablus/ Palestine [77].

2.2 Instrumentation

The instruments used in this research are: pH meter (model: 3510, JENWAY), shaking water bath (Daihan Labtech, 20 to 250 rpm Digital Speed Control), balance (Ohaus corp, item No AR 3130), FT-IR Spectrometer (Thermo Fisher Scientific, Waltham, MA, USA) which equipped with the Smart Split Peaks Hemi Micro ATR accessory (International Crystal Laboratories, Garfield, NJ, USA), Inductively Coupled Plasma Mass Spectrometer ICP-MS (ELAN 9000, ICE 3xxx C113500021 v1.30), thermogravimetric analyser (TGA) (Lenovo V520,

China) and Flame Atomic Absorption Spectrometer at 217 nm (ICE 3000 series AA System, Thermo Scientific).

2.3 Methods

Flame Atomic Absorption Spectrometer (FAAs) used to determine the residual metal ions concertation of studied solutions. All analysis studies were performed in triplicate by FAAS and the mean of the three runs was reported. The error range in the experimental data were analyzed using Excel Microsoft software, a certainty interval of 95% was used. The data analysis was performed using the t-test. All variations were considered statistically when $p < 0.05$ for the analysis of t-test. The flame type was air-C_2H_2.

Nicolet 6700 Fourier transform infrared (FT-IR) spectrometer equipped with the Smart Split Pea micro-ATR accessory was used to check and record the functional groups of the produced polymers. The smart Split Peak is an attenuated total reflectance micro sampling accessory. The accessory has a diamond ATR crystal. The following parameters were used: resolution 4 cm^{-1}, spectral range 400-4000 cm^{-1}, number of scans 16.

Thermo-gravimetric analysis (TGA) and differential scanning calorimetry (DSC) measurements were performed using a TG/DSC 1 Star System (Mettler-Toledo) coupled with a MS-Thermostar GSD320 (Pfeiffer Vacuum) Mass Spectrometer. TG/DSC curves were measured with Pt crucibles, in N_2 flow (20 $mLmin^{-1}$) with a heating rate of 5 $^oC\ min^{-1}$ in the range 25-1100 ^oC by a HT1100 oven connected to a MX5 microbalance

(thermostatic at 22 ºC). The STARe software v.10.0 (Mettler Toledo) controlled the process. Changes in sample composition, thermal stability, and Kinetic parameter for chemical reactions in the sample was measured by TGA.

2.4 Polymers preparation

2.4.1 Preparation of Cellulose acetoacetate (Cell-AA)

A 5.0 g of Cellulose (0.15 mol/anhydrous glucose repeat unit) was added to a 1L one necked round bottomed flask containing 500 ml distilled water and stirred magnetically for 2 hr at room temperature. The cellulose was collected from water by suction filtration then suspended in 500 ml methanol for one hour. This process was repeated three times to activate the cellulose and remove water. The activated cellulose was collected by suction filtration then suspend in a 130.0 ml anhydrous DMAc (MM=87.12 g/mol, 1.4 mol) two times, the first time was done for an hour, while the second time was carried out for one night.

A 16.25 g of anhydrous LiCl (MM= 42.394 g/mol, 383.3 mmol) was dissolved in 250 ml of DMAc (2.697 mol) in a 500 ml two round bottomed flask equipped with a magnet stir bar and condenser, the flask was connected to a trap via the condenser and kept under nitrogen gas. The cellulose was collected by suction filtration and transferred to the two necked round bottomed flask which contain a dissolved solution of LiCl/DMAc and stirred until clear solution was obtained (required three hours). After that a 33.5 ml of a t-BAA (9.6 g, 61.5 m.mol) was added

dropwise to the solution under protective nitrogen, then the solution was heated to 120 ºC using oil bath in two hr, and stirred overnight. The reaction was transferred to a 1L beaker, then 800 ml of distilled water was added dropwise to the reaction and then placed in the refrigerator overnight.

The resulted gel was filtered by suction filtration then transferred to 1000 ml beaker containing 500 ml of methanol then stirred for washing. This step repeated twice, the first stirring was done for 15 min, while the second one was carried out for 30 min, after that filtered and dried at 100 ºC in oven until water evaporate completely.

FT-IR spectrum shows the presence of two peaks at 1720-1750 cm^{-1}, which corresponding to the C=O of ester and ketone groups.

2.4.2 Preparation of cellulose β-aminoester using aniline (Cell-β-AN)

A 2.0 g of cell-AA polymer suspend in 100 ml methanol, then 2 ml (2.04 g, 21.9 mmol) of aniline was added immediately, after that 2 ml (2.1 g, 34.96 mmol) of acetic acid was added at once as a catalyst to the reaction. Reflux was done for 8 hr at 80 ºC. The resulted polymer was filtered and dried in oven at 110 ºC until acetic acid evaporated completely.

FT-IR spectrum shows the presence of a peak at 3300-3500 cm^{-1}, which corresponding to the N-H stretching of an amine group in addition to the ester peak at 1740 cm^{-1}.

2.4.3 Preparation of cellulose β-aminoester using glycine (Cell-β-GL)

A 2.0 g of cell-AA polymer suspend in 40 ml methanol, then 2.0 g (1.587 ml, 26.6 mmol) of glycine was added immediately. Reflux was done for 6 hr at 70 ºC. The resulted polymer was washed two times with water then two times with methanol, after that filtered and dried in oven at 90 ºC until methanol evaporate completely.

FT-IR spectrum shows the presence of a peak at 3300-3500 cm^{-1}, which corresponding to the N-H stretching of an amine group and 1740 and 1670 cm^{-1} two peaks corresponding to the carbonyls of ester and carboxylic acid, respectively.

2.4.4 Polymer solubility in water

A 0.5 g of each of the polymers prepared above was suspended in 50 ml water and stirred for about 6 hrs. Then collected by suction filtration, dried in an oven at 100 ^{o}C, and weighed. Negligible reduction in the weight was noticed.

2.5 purification of contaminated water from lead metal using Cellulose polymer

2.5.1 preparation of lead solutions

A stock solution of lead nitrate with a 1000 ppm concentration was prepared at the lab by dissolving 1.5985 g of $Pb(NO_3)_2$ (MM = 331.21 g/mol) in a one Liter volumetric flask. Then several standard solutions with various concentrations ranged from 1.0 to 50.0 ppm were prepared from the stock.

These standard solutions were used to create the calibration curve and to study the effect of different factors such as: initial concentrations, dosage, time, pH and temperature on the efficiency of polymers adsorbing heavy metal.

The adsorption of all studied solutions was measured by Flame Atomic Absorption spectroscopy at 217 nm. The solutions were used to create the calibration curves for Pb(II) ions by measuring the absorbency of the standard solutions. Based on the resulting calibration curves, the residual lead ions concentrations in the filtered samples were calculated.

2.5.2 Calibration Curves

Flame atomic absorption spectroscopy (FAAS) was used to create the calibration curves for Pb(II) by measuring the absorbency of the standard solutions.

The calibration curve for Pb(II) is shown in Figures 2.1.

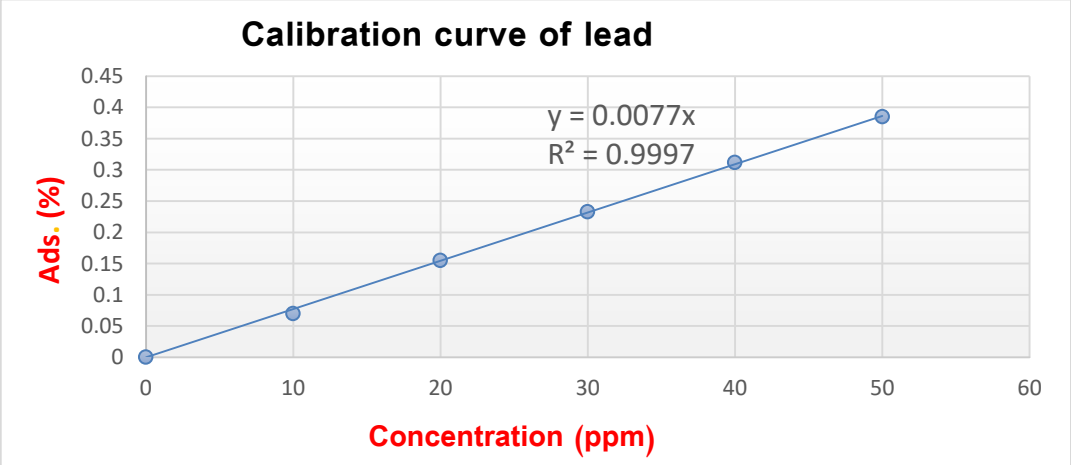

Fig (2.1): Calibration curve of Pb(II)

2.5.3 Batch Adsorption Experiments

General procedure

A sample with known amount of cellulose-based polymer was added to a specific volume of lead solution with known concentration in a bottle, then the bottle was closed and shake in the shaker apparatus at constant pH, temperature and at a speed of 125 periods/min for a specific period of time according to the factor which is under study. A sample of each mixture was withdrawn by a syringe, then filtered through a 0.45 µm syringe filter. The filtered sample analyzed by atomic absorption spectroscopy for determining the residual metal ions concentrations and thus to know the efficiency of adsorption.

2.5.3.1 Effect of adsorbent weight (dosage) on the removal efficiency

For determining the optimum amount of adsorbent in the adsorption of Pb(II) on modified cellulose, different quantities of cellulose based-polymer (10.0, 20.0, 30.0, 40.0, 50.0 mg) were added to six vials containing 10 ml of 10 ppm standard solution of the metal ion.

Then these solutions were shaken for 30 minutes using thermostat shaker at constant temperature of 25 ºC and 4.3 pH, after the shaking time end, a sample of each mixture was withdrawn with a syringe, filtered through a 0.45 µm syringe filter and subjected to analysis for residual metal ions concentrations by FAAs.

The adsorption efficiency of the prepared three polymers (cell-AA, Cell-β-GL, Cell-β-AN) were evaluated in the same manner. The obtained results for three polymers are summarized in tables 2.1, 2.2 and 2.3:

Table (2.1): Effect of polymer dose on the Pb(II) removal efficiency for polymer Cell-AA under 10 ppm of Pb(II) for 30 min at 25 ºC and 4.3 pH.

Polymer dose (mg)	$[Pb^{2+}]$ (ppm)	% Removal of Pb^{2+}
5	9.159	8.410
10	8.798	12.024
20	8.531	14.687
30	7.578	24.217
40	5.915	40.848
50	5.565	44.353

Table (2.2): Effect of polymer dose on the Pb(II) removal efficiency for polymer Cell-β-AN under 10 ppm of Pb(II) for 30 min at 25 ºC and 4.3 pH

Polymer dose (mg)	$[Pb^{2+}]$ (ppm)	% Removal of Pb^{2+}
5	4.889	51.109
10	4.883	51.172
20	4.996	50.037
30	4.879	51.215
40	4.694	53.059
50	4.271	57.292

Table (2.3): Effect of polymer dose on the Pb(II) removal efficiency for polymer Cell-β-GL under 10 ppm of Pb(II) for 30 min at 25 ºC and 4.3 pH

Polymer dose (mg)	$[Pb^{2+}]$ (ppm)	% Removal of Pb^{2+}
5	7.923	20.774
10	7.762	22.385
20	6.506	34.938
30	5.847	41.531
40	3.950	60.498
50	3.629	63.711

2.5.3.2 Effect of contact time on the lead (Pb^{2+}) removal efficiency

The adsorption of the metal ions on each adsorbent was studied as a function of contact time at the optimum dosage of polymer and adsorbate concentration. Six solutions (10 ml each) of lead nitrate with concentration (10 ppm) were put in six vials, then 50.0 mg of Cell-AA polymer dosage that gave maximum removal efficiency added to each, then the solutions were shaken at 25 ºC and 4.3 pH for different times (1 min, 10 min, 20 min, 30 min, 1hr, 2hr, 3hr). At the end of each time interval, each sample was withdrawn with a syringe, filtered through a 0.45 µm syringe filter and subjected to analysis for residual metal ions concentrations by FAAs. These steps were repeated for Cell-β-GL and Cell-β-AN polymers.

The adsorption efficiency of the prepared three polymers Cell-AA, Cell-β-AN, and Cell-β-GL as a function of time were all evaluated in the same manner. The obtained results for three polymers are summarized in the following tables:

Table (2.4): Effect of contact time on the lead Pb(II) removal efficiency for polymer Cell-AA under 10 ppm of Pb(II), 50 mg of the polymer at 25 ºC and 4.3 pH.

Contact time (min)	$[Pb^{2+}]$ (ppm)	% Removal of Pb^{2+}
1	8.876	11.237
10	8.456	15.442
20	7.841	21.594
30	7.452	25.485
60	7.148	28.525
120	5.189	48.111
180	4.924	50.757

Table (2.5): Effect of contact time on the Pb(II) removal efficiency for polymer Cell-β-AN under 10 ppm of Pb(II), 50 mg of the polymer at 25 ºC and 4.3 pH.

Contact time (min)	[Pb^{2+}] (ppm)	% Removal of Pb^{2+}
1	5.432	45.682
10	5.031	49.692
20	5.159	48.410
30	4.271	57.292
60	4.500	55.000
120	4.701	52.990
180	4.600	54.000

Table (2.6): Effect of contact time on the Pb(II) removal efficiency for polymer Cell-β-GL under 10 ppm of Pb(II), 50 mg of the polymer at 25 ºC and 4.3 pH.

Contact time (min)	[Pb^{2+}] (ppm)	% Removal of Pb^{2+}
1	6.369	36.308
10	6.209	37.906
20	5.444	45.564
30	4.782	52.181
60	4.396	56.038
120	3.230	67.698
180	3.029	69.705

2.5.3.3 Effect of temperature on lead (Pb^{2+}) removal efficiency

For studying the effect of temperature on the adsorption process, five solutions (10 ml each) of lead nitrate with concentration (10 ppm) and 4.3 pH were placed in five vials, 50.0 mg of Cell-AA polymer was added to the solutions and placed in shaking water bath, for 30 min at the desired temperatures (15 ºC, 22 ºC, 30 ºC, 40 ºC and 60 ºC).

At the end of each experiment the sample of each mixture was withdrawn with a syringe, filtered through a 0.45 µm syringe filter and subjected to analysis for residual metal ions concentrations by FAAs. These steps were repeated for Cell-β-GL and Cell-β-AN polymers.

The adsorption efficiency of the prepared three polymers Cell-AA, Cell-β-AN, and Cell-β-GL as a function of temperature were evaluated in the same manner. The obtained results for three polymers are summarized in the following tables:

Table(2.7): Effect of temperature on the Pb(II) removal efficiency for polymer Cell-AA under 10 ppm of Pb(II), 50 mg of the polymer, 4.3 pH for 30 min

Temperature (ºC)	$[Pb^{2+}]$ (ppm)	% Removal of Pb^{2+}
15	7.739	22.632
22	7.841	21.594
30	5.565	44.353
40	7.411	25.895
60	7.873	21.274

Table(2.8): Effect of temperature on the Pb(II) removal efficiency for polymer Cell-β-AN under 10 ppm of Pb(II), 50 mg of the polymer, 4.3 pH for 30 min

Temperature (ºC)	$[Pb^{2+}]$ (ppm)	% Removal of Pb^{2+}
15	5.205	47.947
22	5.086	49.142
30	4.271	57.292
40	6.514	34.865
60	7.385	26.149

Table (2.9): Effect of temperature on the Pb(II) removal efficiency for polymer Cell-β-GL under 10 ppm of Pb(II), 50 mg of the polymer, 4.3 pH for 30 min

Temperature (ºC)	[Pb^{2+}] (ppm)	% Removal of Pb^{2+}
15	4.957	50.433
22	4.782	52.181
30	3.629	63.711
40	4.545	54.553
60	5.214	47.860

2.5.3.4 Effect of lead nitrate concentration on removal efficiency

To find out the optimum concentration of lead Pb^{+2} ions, five different lead nitrate standard solutions were prepared from stock solution (1000 ppm). The standard solution concentrations (10, 20, 30, 40 and 50 ppm). The optimum dose (50.0 mg) of each polymer was added to five vials each containing 10.0 ml of different standard solution of Pb^{+2}. The pH 4.3, time 30 min and temperature 25.0 ºC were kept constant for the five samples. Then the sample of each mixture was withdrawn with a syringe, filtered through a 0.45 µm syringe filter and subjected to analysis for residual metal ions concentrations by FAAs.

The adsorption efficiency of the prepared three polymers Cell-AA, Cell-β-AN, and Cell-β-GL as a function of Lead(II) concentration were evaluated in the same manner. The obtained results for three polymers are summarized in the following tables:

Table (2.10): Lead nitrate concentration effect on Pb(II) removal efficiency for polymer Cell-AA under 50 mg of the polymer, at 25 ºC and 4.3 pH for 30 min

Lead nitrate Concentration (ppm)	$[Pb^{2+}]$ (ppm)	% Removal of Pb^{2+}
10	5.565	44.353
20	14.606	26.974
30	28.646	4.515
40	38.772	3.070
50	46.431	7.138

Table (2.11): Lead nitrate concentration effect on Pb(II) removal efficiency for polymer Cell-β-AN under 50 mg of the polymer, at 25 ºC and 4.3 pH for 30 min

Lead nitrate Concentration (ppm)	$[Pb^{2+}]$ (ppm)	% Removal of Pb^{2+}
10	4.271	57.292
20	16.334	18.333
30	30.000	0.000
40	40.000	0.000
50	47.951	4.099

Table (2.12): Lead nitrate concentration effect on Pb(II) removal efficiency for polymer Cell-β-GL under 50 mg of the polymer, at 25 ºC and 4.3 pH for 30 min.

Lead nitrate Concentration (ppm)	$[Pb^{2+}]$ (ppm)	% Removal of Pb^{2+}
10	3.629	63.711
20	12.975	35.124
30	25.611	14.631
40	36.455	8.863
50	43.056	13.889

2.5.3.5 Effect of pH on the efficiency of lead removal

Adsorption was studied at different pH values ranging from 3-12 to determine the effect of pH on the adsorption process. Six solutions of lead nitrate (10 ppm concentration each) were prepared. Their pH were adjusted to the desired pH values using either 0.1 M HCl or 0.1 M NaOH solutions and diluted solutions of HCl and NaOH. The temperature 25.0 ºC were kept constant for the six samples. 50.0 mg of adsorbent were added to 10 ml of the 10.0 ppm standard solutions and placed in shaking water bath, for 30 min.

At the end of each experiment the sample of each mixture was withdrawn with a syringe, filtered through a 0.45 µm syringe filter and subjected to analysis for residual metal ions concentrations by FAAs.

The adsorption efficiency of the prepared three polymers Cell-AA, Cell-β-AN, and Cell-β-GL as a function of pH were evaluated in the same manner. The obtained results for three polymers are summarized in the following tables:

Table (2.13): Effect of pH on the Pb(II) removal efficiency for polymer Cell-AA under 10 ppm of Pb(II), 50 mg of the polymer, at 25 ºC for 30 min.

pH	$[Pb^{2+}]$ (ppm)	% Removal of Pb^{2+}
3	10.000	0.000
4.5	6.380	36.197
6	3.194	68.059
7	1.979	80.214
9	0.510	94.897
11.5	1.328	86.720

Table (2.14): Effect of pH on the Pb(II) removal efficiency for polymer Cell-β-AN under 10 ppm of Pb(II), 50 mg of the polymer, at 25 ºC for 30 min.

pH	$[Pb^{2+}]$ (ppm)	% of Pb^{2+} removal
3	9.852	1.479
4.5	5.700	43.000
6	3.459	65.411
7	2.669	73.310
9	1.327	86.727
11.5	3.279	67.211

Table (2.15): Effect of pH on the Pb(II) removal efficiency for polymer Cell-β-GL under 10 ppm of Pb(II), 50 mg of the polymer, at 25 ºC for 30 min.

pH	$[Pb^{2+}]$ (ppm)	% Removal of Pb^{2+}
3	9.219	7.811
4.5	4.851	51.493
6	2.082	79.185
7	0.823	91.775
9	0.838	91.620
11.5	1.583	84.169

2.5.3.6 Polymer adsorption cycle

The polymer recycling is an important factor to have a more sustainable, and cost-effective process. The polymer efficiency after using was studied by using the used polymer for another adsorption process under optimized condition. For that, about 100.0 mg of each adsorbents were loaded with 10 mL of 10.0 ppm of lead nitrate solutions and the solutions were adjusted to a pH value 9.0, shaken for 30 min at room temperature. The supernatant was separated from adsorbent by syringe with small needle (0.30 x 13mm), then filtered through a 0.45 µm syringe filter and subjected to analysis for

residual lead ions concentrations by FAAs. The collected 100 mg of adsorbent was added to 10 ml of water and the pH value was adjusted to 3.0 with 0.1 M hydrochloric acid and shaken for 20 min to remove adsorbed metal ions, next the solutions were decanted. These steps were repeated for seven times to detect if the used polymer still have efficiency for removal lead ion from contaminated water or not.

The results for the seven used polymers are summarized in the following tables:

Table (2.16): Recycling of polymer Cell-AA under 10 ppm of Pb(II), 100 mg of the polymer, for 30 min at 25 ºC and 9 pH

Number of reusing	Concentration of lead (Pb^{2+}) after extraction	% of extraction
1	0.000	100.000
2	0.000	100.000
3	0.009	99.910
4	0.021	99.787
5	0.059	99.410
6	0.073	99.270
7	0.096	99.040

Table (2.17): Recycling for polymer Cell-β-AN under 10 ppm of Pb(II), 100 mg of the polymer, for 30 min at 25 ºC and 9 pH

Number of reusing	Concentration of lead (Pb^{2+}) after extraction	% of extraction
1	0.000	100.000
2	0.001	99.990
3	0.020	99.800
4	0.053	99.470
5	0.094	99.060
6	0.100	99.000
7	0.130	98.700

Table (2.18): Recycling for polymer Cell-β-GL under 10 ppm of Pb(II), 100 mg of the polymer, for 30 min at 25 ºC and 9 pH

Number of reusing	Concentration of lead (Pb^{2+}) after extraction	% of extraction
1	0.000	100.000
2	0.020	99.800
3	0.050	99.500
4	0.102	98.980
5	0.114	98.860
6	0.132	98.680
7	0.150	98.500

2.6 Wastewater Purification

A sample of sewage water collected from the Beit Dajan wastewater purification planet (Nablus-Palestine) was used in this study. The sample was subject to analysis by ICP-AES (the analysis was performed by the Water Center at An-Najah National University, Nablus, Palestine) to determine the metals content and their concentrations. Three 20 ml samples of the wastewater were placed in three Erlenmeyer flasks, then 0.2 g of each cellulose-based polymer (Cell-AA, Cell-β-AN, Cell-β-GL) was added to each sample. The mixtures were shaken at room temperature for 120 min using thermostat shaker. Next 0.5 ml of nitric acid (70% purity) was added to each sample for dissolution any biological material. A sample of each mixture was withdrawn with a syringe and filtered through a 0.45 µm syringe filter and subjected to analysis by ICP-AES for residual metal ions concentrations.

Chapter Three

Results and Disscusion

3.1 Synthesis of cellulose-acetoacetate polymers

In this work, three polymers were synthesized, developed and used in waste water purification from toxic metal ions. The materials used for this purpose were cellulose, glycine and aniline. Cellulose and glycine are natural, commercially available, cheap and environmentally friendly.

Cellulose can't be dissolved in common organic solvent due to the presence of a strong hydrogen bond between polymer chains. To dissolve cellulose, the network of hydrogen bonds must be broken, and this is achieved by dissolving cellulose in solvents such as N,N-dimethylacetamide/Lithium chloride (DMAc/LiCl). The mixture of LiCl (8 wt.%)/DMAc forms a complex between lithium and DMAc with a free chloride anion, $[Li{\cdot}xDMAc]^{+}Cl^{-}$. This solution dissolve cellulose by breaking the inter-chain H-bonding and bind strongly to the hydroxyl groups of cellulose. DMAc/LiCl is environmentally friendly solvent and cellulose dissolves in LiCl/ DMAc with no degradation [92].

In DMAc/LiCl mixture, LiCl presence in the Li^{+}-Cl^{-} ion pair form. When cellulose dissolved in DMAc/LiCl, the free chloride anions participate in dissolution by weakness the hydrogen bond of cellulose. The intermolecular hydrogen bonds between cellulose chains are replaced with a with strong dipole-dipole interaction between cellulose hydroxyl group and Cl^{-} ($OH\ldots Cl^{-}$). The Li^{+} cations bind strongly with the carbonyl oxygen

in DMAc molecule to form Li^{+}(DMAc) complex as shown in fig 3.1 [93,94]. This way the cellulose chains get dispersed in the solvent to form clear viscose solution.

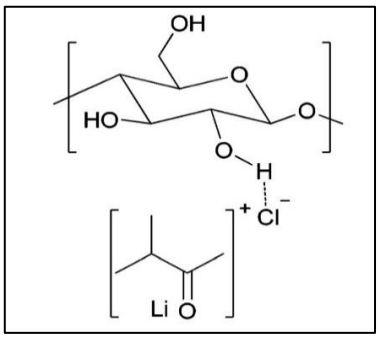

Fig (3.1): A representative figure the interaction between cellulose and LiCl/ DMAc

Cellulose is a trivalent polymeric alcohol (contain three hydroxyl groups). The primary hydroxyl group at C6 have relatively low steric hindrance, the secondary hydroxyl group at C2 have relatively high acidity. Because of this, the ingrained reactivity of the three hydroxyl groups at the cellulose backbone is different. The esterification reactions are selective for the less hindered primary hydroxyl group [95].

The t-BAA undergoes transesterification with primary alcohol at cellulose dissolved in DMAc/LiCl solvent to form cellulose acetoacetate. The reaction is performed at 120 ºC and under N_2 gas in a catalyst-free system which could related to the presence of the t-Butyl leaving group as shown in schematic 3.1.

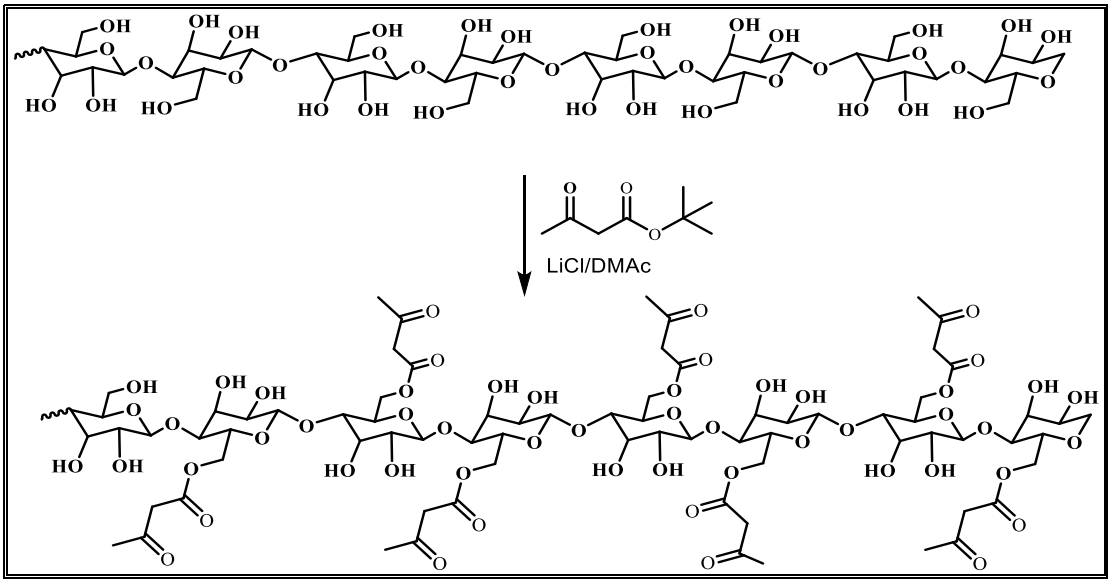

Schematic (3.1): preparation of cellulose acetoacetate from Cellulose

This reaction protocol is only restricted to tert-butyl beta-ketoester [96]. The hindered t-BAA is more reactive than the commonly used methyl or ethyl analogs. Nitrogen gas used to protect the reaction from oxygen and humidity since presence of water lead to undesirable base hydrolysis. According to le'Chatellier principle, if water is added to the reaction, it will derive the reaction toward the reagent (in the backwards direction). Isolation and purification of β- ketoeaster is achieved by heating the reaction for six hours under reflux.

The mechanism of the transesterification reaction is shown in Figure 3.2. The hydroxyl group undergoes nucleophilic attach on the ester carbonyl carbon in t-BAA with loss of proton and t-butoxide the target cellulose acetoacetate produced.

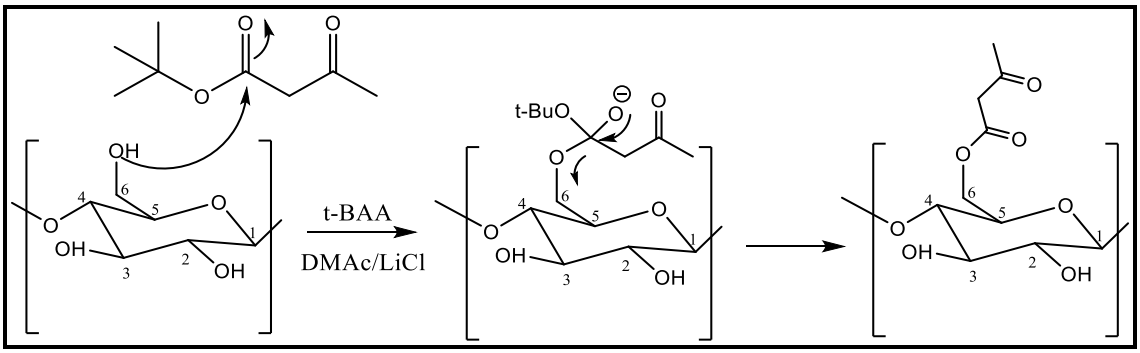

Fig (3.2): Mechanism of transesterification of NCC

3.1.1 FT-IR of cellulose and Cellulose acetoacetate

The FT-IR spectra of untreated cellulose (Figure 3.3) shows a broad peak at 3337 cm^{-1} attributed to the stretching of hydrogen bonded hydroxyl group (O-H). The peak at 1316 cm^{-1} could be related to the O-H bending vibration. The adsorption peak at about 2900 cm^{-1} is corresponding to the symmetric and asymmetric stretching vibration of the C-H bond. The 1430 cm^{-1} band resulted from CH_2 asymmetric bending. The IR spectrum also shows a peak at 1057 cm^{-1} that could be attributed to the C-O-C pyranose ring skeletal vibration, and peak at 1033 cm^{-1} corresponding to β-glycosidic linkage.

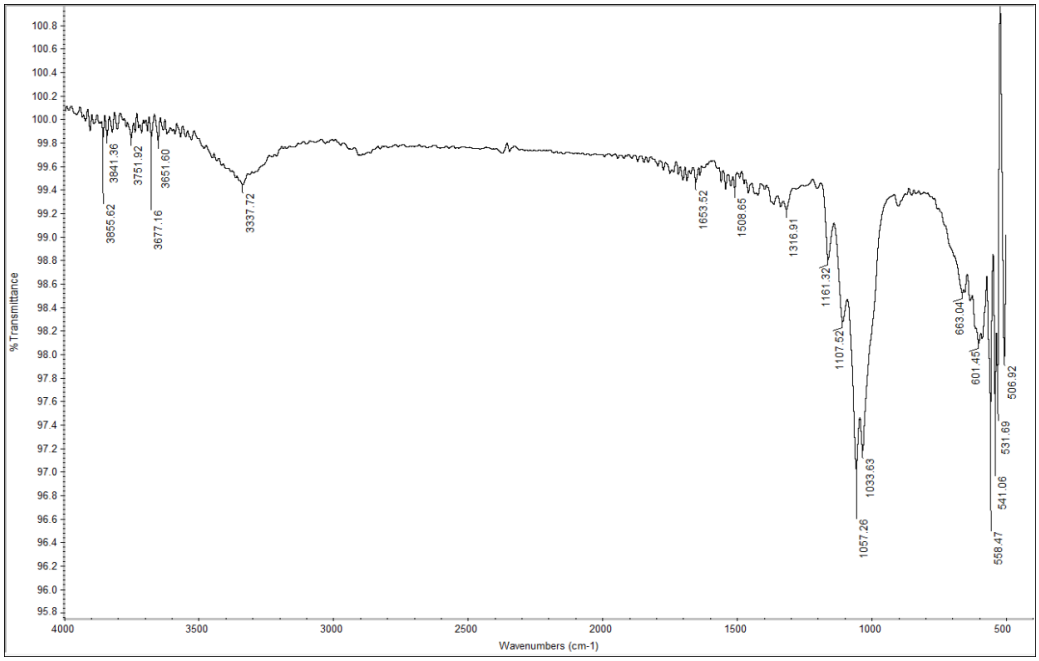

Fig (3.3): FT-IR spectrum for cellulose

The FT-IR spectrum of the cellulose acetoacetate is shown in Figure 3.4. The most significance sharp peaks for Cell-AA were observed at 1742 and 1709 cm^{-1} assigned to the typical C=O (ester) and C=O (ketone) stretching, respectively. The IR spectrum of the product shows three bands at about 1152, 1057 and 1033 cm^{-1} for C-O-C of ester, pyranose ring skeletal and to β-glycosidic linkage vibration, respectively. The broad peak at 3439 cm^{-1} attributed to hydrogen bonded hydroxyl group (O-H) stretching. The adsorption peak at about 2900 cm^{-1} is corresponding to the symmetric and asymmetric stretching vibration of the C-H bond. The peak at 1418 cm^{-1} resulted from C-H bending vibration.

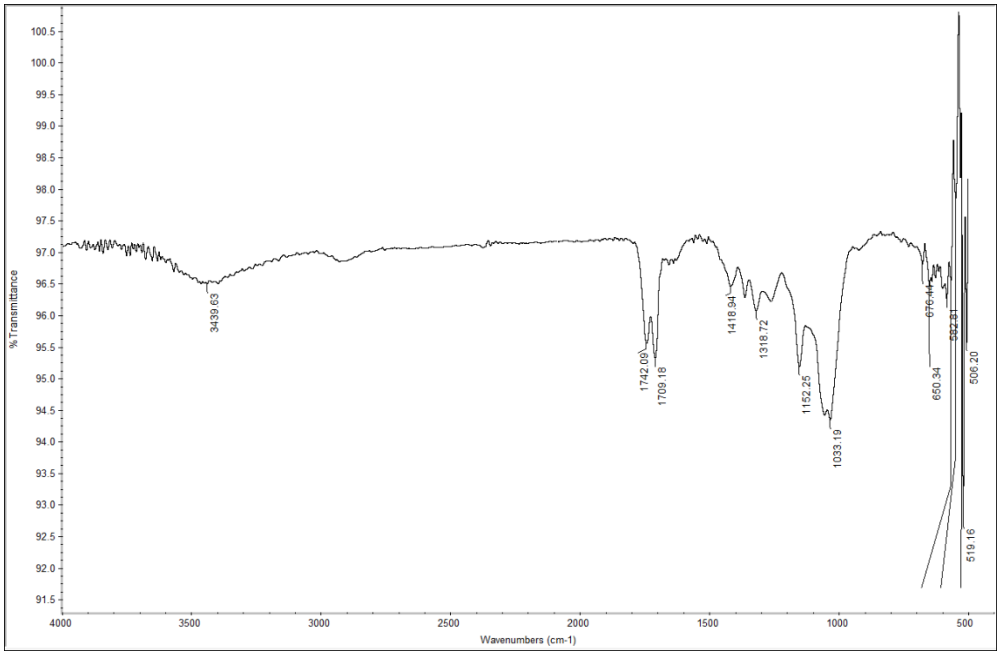

Fig (3.4): FT-IR spectrum for Cell-AA

3.1.2 TGA analysis and thermal stability

The thermal analysis was performed under air with a heating rate of 20 ºC per min during the analysis. The results of TGA analysis of Cell-AA is shown in figure 3.5.

The results show big drop in the mass at 200 ^{o}C that could be related to the loss of the acetoacetate functional group. Complete decomposition of the of the polymer stated at about 450 ^{o}C. The polymer is considered thermally ? since it synthesized mainly for waste water purification.

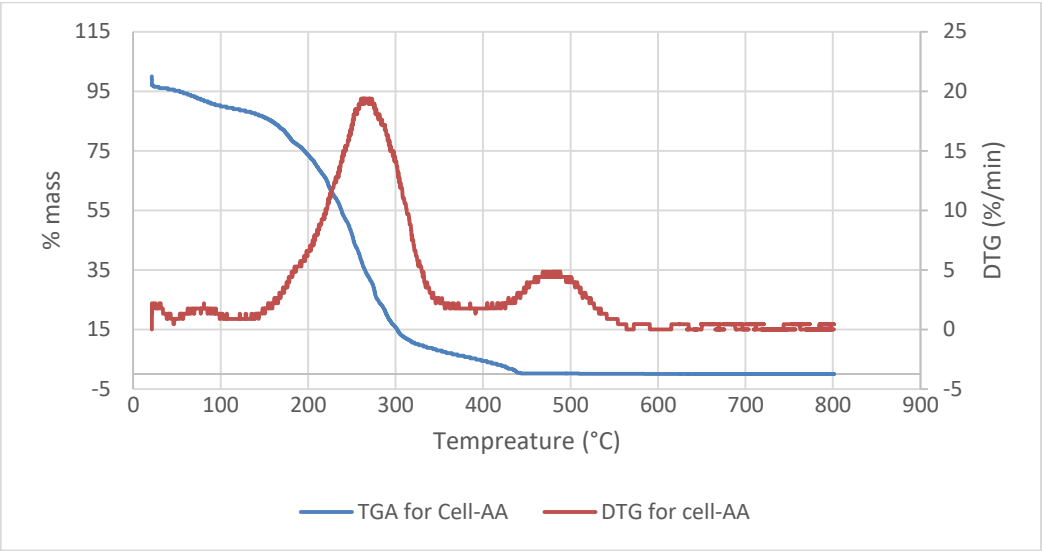

Fig (3.5): TGA and DTG analysis for Cell-AA polymer.

3.2 Synthesis of cellulose β-aminoester using aniline

Cellulose β-aminoester was produced by reacting cellulose acetoacetate with aniline dissolved in methanol in presence of acetic acid as a catalyst as shown in Figure 3.6. Aniline is a primary aromatic amine act as a nucleophile that attacks the electrophilic carbonyl group of ketone in cellulose acetoacetate to form an intermediate. This intermediate is protonated to remove the negative charge from the oxygen. Next this intermediate is deprotonated to give carbinolamine (hemiaminal). Acid protonation of the carbinolamine oxygen convert it to a good leaving group then water molecules is eliminated. After the departure of water molecules, iminium ions are formed which stabilized by resonance as shown in Figure 3.7. Deprotonation of iminium ion gives the final cellulose β-aminoester that is known as Schiff base.

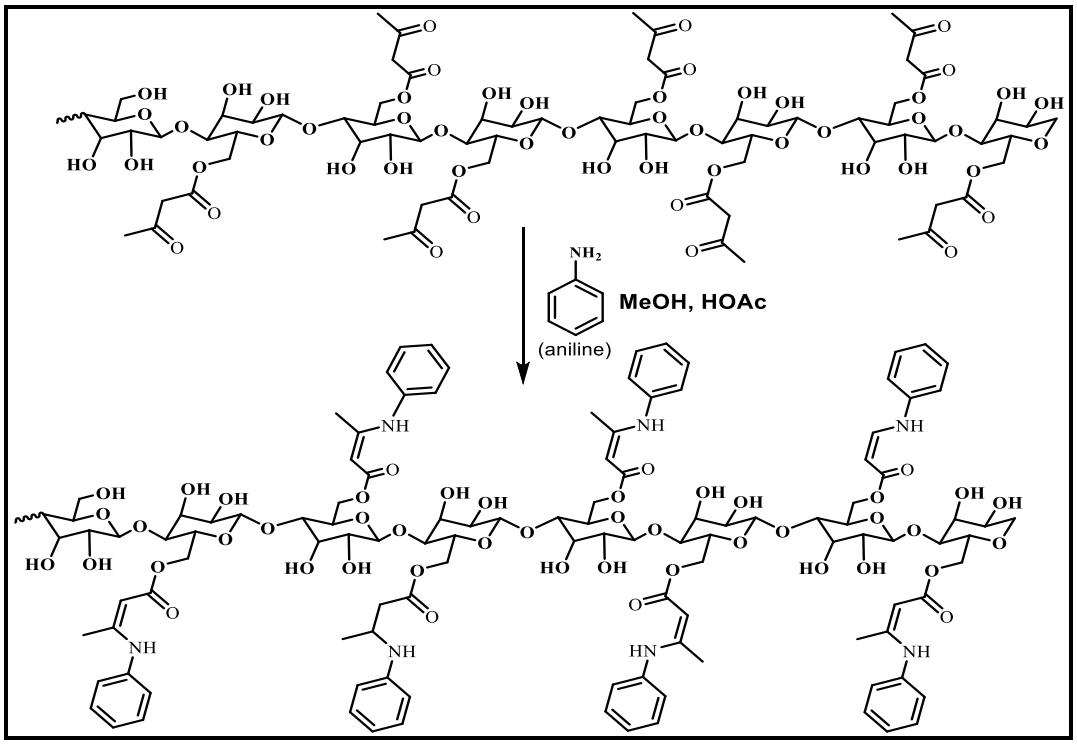

Figure (3.6): Preparation of cellulose β-anilinoacetonate (Cell-β-AN) using aniline

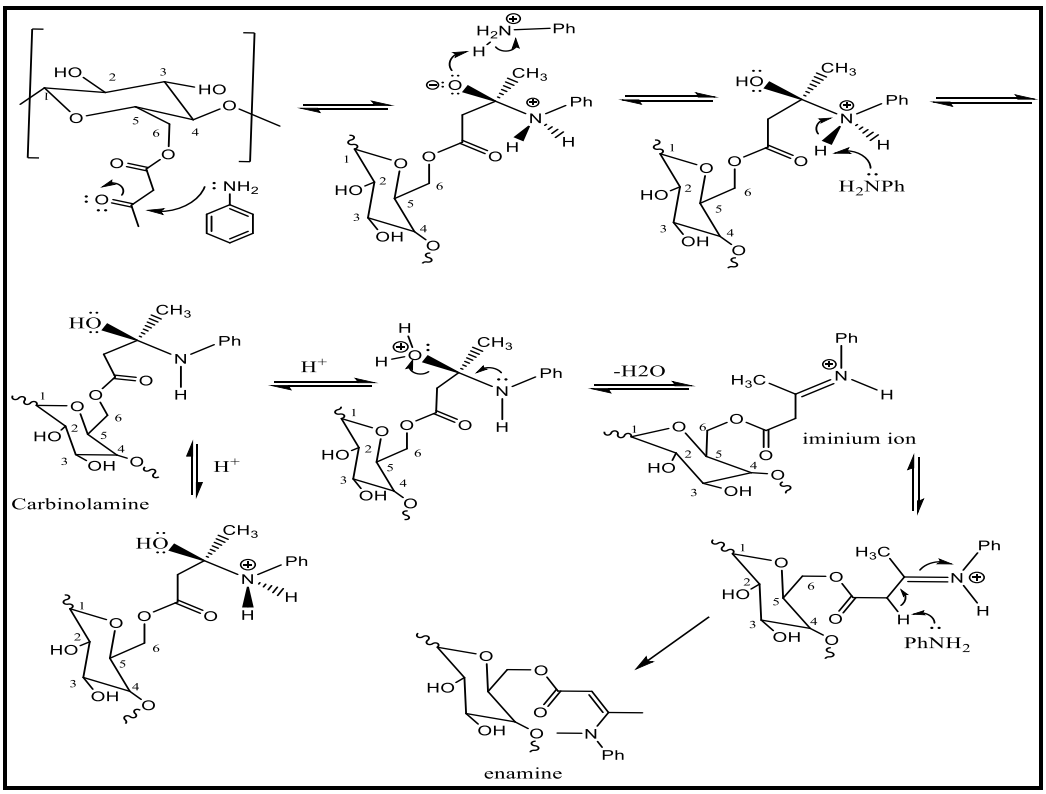

Fig 3.7: Reaction mechanism for the synthesis of cellulose β-anilinoacetonate.

3.2.1 FT-IR of cellulose β-anilinoacetonate

Figure 3.8 shows the FT-IR spectrum of aniline. Two small, sharp bands positioned at around 3440, 3351 cm^{-1} were detected, which corresponding to the primary N-H stretching of aniline molecule. Note that the shoulder band at 3212 is an overtone of the N-H bending vibration. The small, sharp band at 3033 cm^{-1} resulted from aryl C-H stretching vibration. The C-N stretching band appears at 1271 cm^{-1}. Also, the two adsorptions peak at 1618 and at 1495 corresponding to N-H bending and C-C stretching vibration, respectively. The 1599 cm^{-1} is corresponding to aromatic C=C stretching.

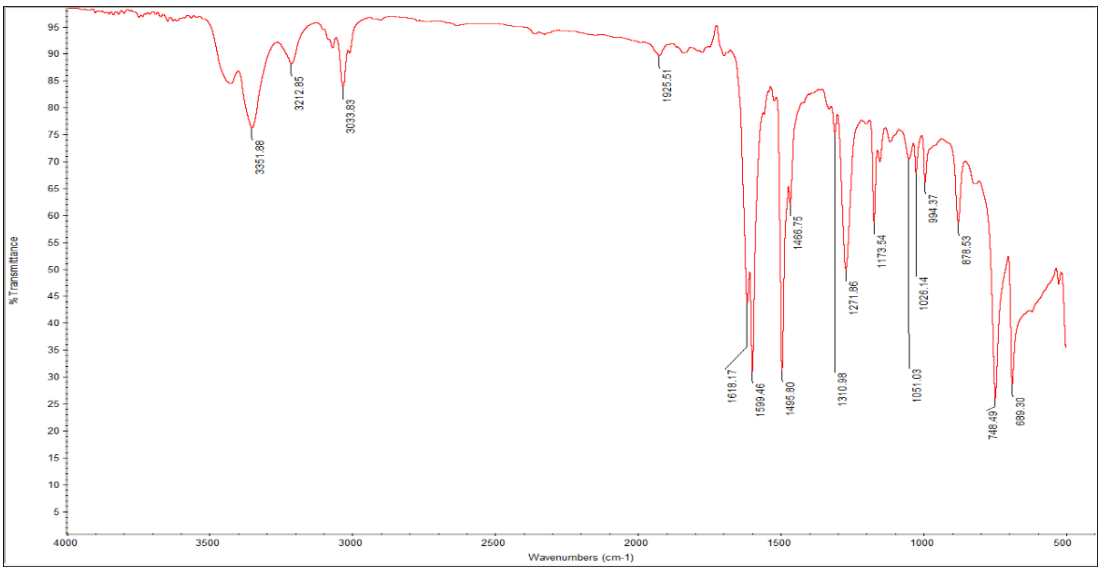

Fig (3.8): The FT-IR spectrum of aniline

The FT-IR spectrum of the Cell-β-AN is shown in Figure 3.9. The disappearance of the ketone domain at 1709 and the presence of an amine group C-N at about 1271 cm^{-1} is an indication that the amine linkage is formed. The peak at 3473 cm^{-1} is due to N-H vibration of the secondary amine groups. The peak at 1740 cm^{-1} attributed to C=O of ester group. The

presence of these carbonyl and amine groups is important for metal ion trapping. The broad peak at 3430 cm^{-1} attributed to hydrogen bonded hydroxyl group (OH) stretching. The amine peak is not sharp, because it overlaps with the OH group peak which have almost the same range, so the N-H amine signal is imprecise. The IR spectrum shows three bands at about 1157, 1055 and 1033 cm^{-1} for C-O-C of ester, pyranose ring skeletal and to β-glycosidic linkage vibration respectively. The adsorption peak at 2922 cm^{-1} actually is corresponding to symmetric and asymmetric stretching vibration of the C-H bond. The peak at 1420 cm^{-1} resulted from C-H bending vibration. The two peaks at about 3010 and 1582 cm^{-1} attributed to =C-H and C=C stretching vibrations in an aromatic part of Cell-β-AN.

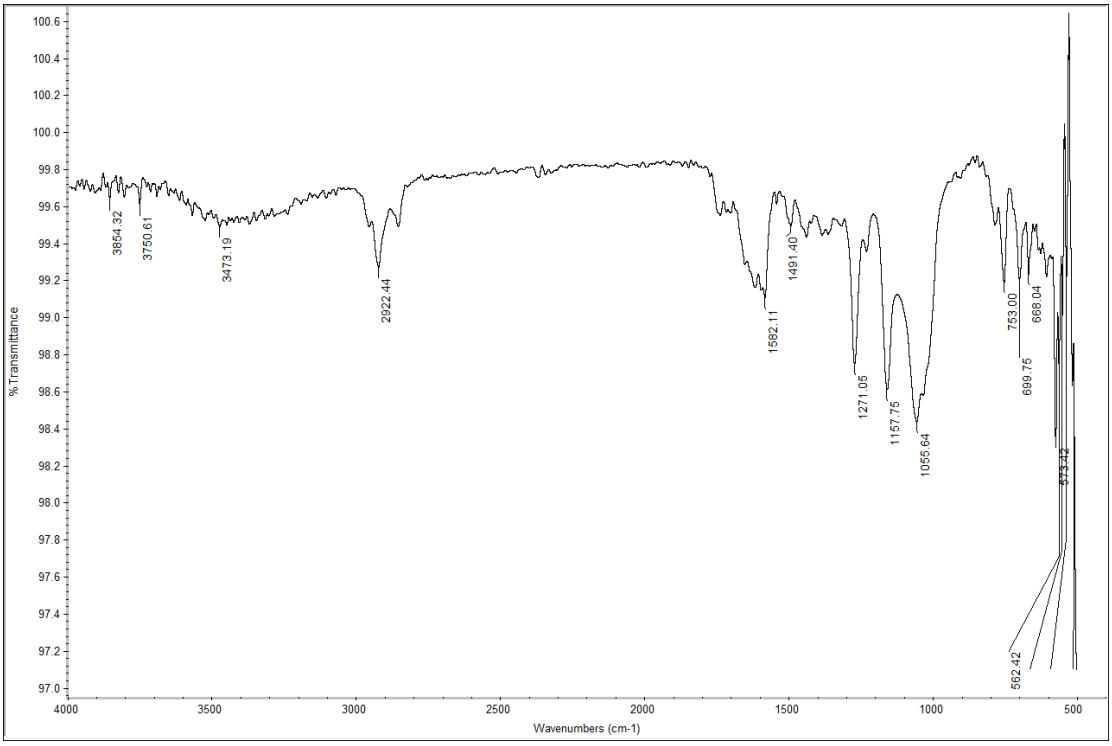

Fig (3.9): FT-IR spectrum for Cell-β-AN

3.2.2 TGA analysis and thermal stability of Cell-β-AN

The thermal analysis was performed under air with a heating rate of 20 ºC per min during the analysis. The results of TGA analysis of Cell-β-AN is shown in figure 3.10.

The results show a small drop in the mass at about a 100 ^{o}C due to dehydration. A big drop in the mass started at about 180 ^{o}C which could be attributed to the loss of the anilinoacetate group. Complete decomposition of the of the polymer stated at about 450 ^{o}C. Again, the polymer is thermally stable considering the main purpose of making it which is wastewater purification.

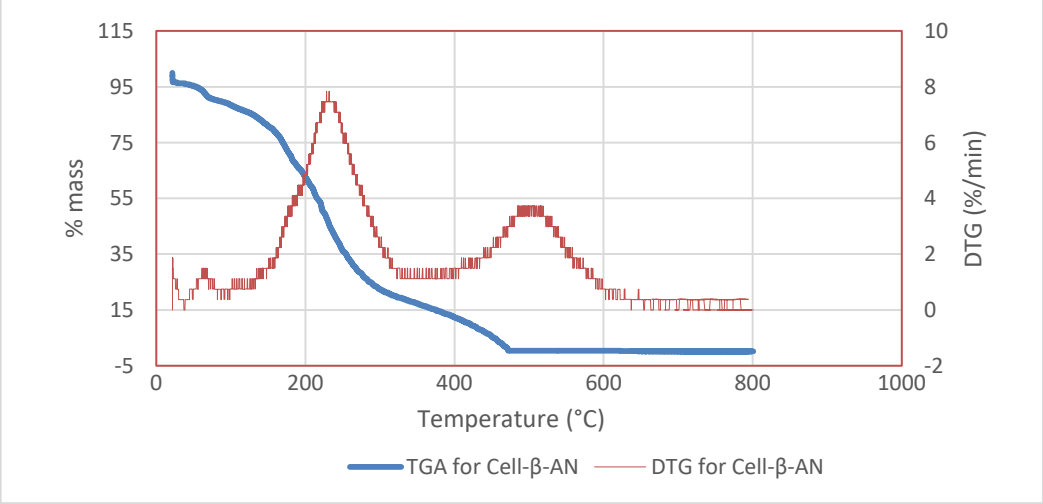

Fig (3.10): TGA and DTG analysis for Cell-β-AN polymer

3.3 Synthesis of cellulose β-glycineacetoester (Cell-β-GL)

The cellulose β-aminoester was produced by reacting cellulose acetoacetate with the amino acid glycine, acetic acid was used as a solvent and catalyst. The reaction is depicted in figure 3.11. Glycine is a primary aliphatic amine act as a nucleophile that attacks the electrophilic carbonyl group of ketone

in cellulose acetoacetate. The mechanism of reaction is the same as that shown for aniline (Figure 3.7) with cellulose acetoacetate. The reaction mechanism of glycine and cellulose acetoacetate is shown in the Figure 3.11.

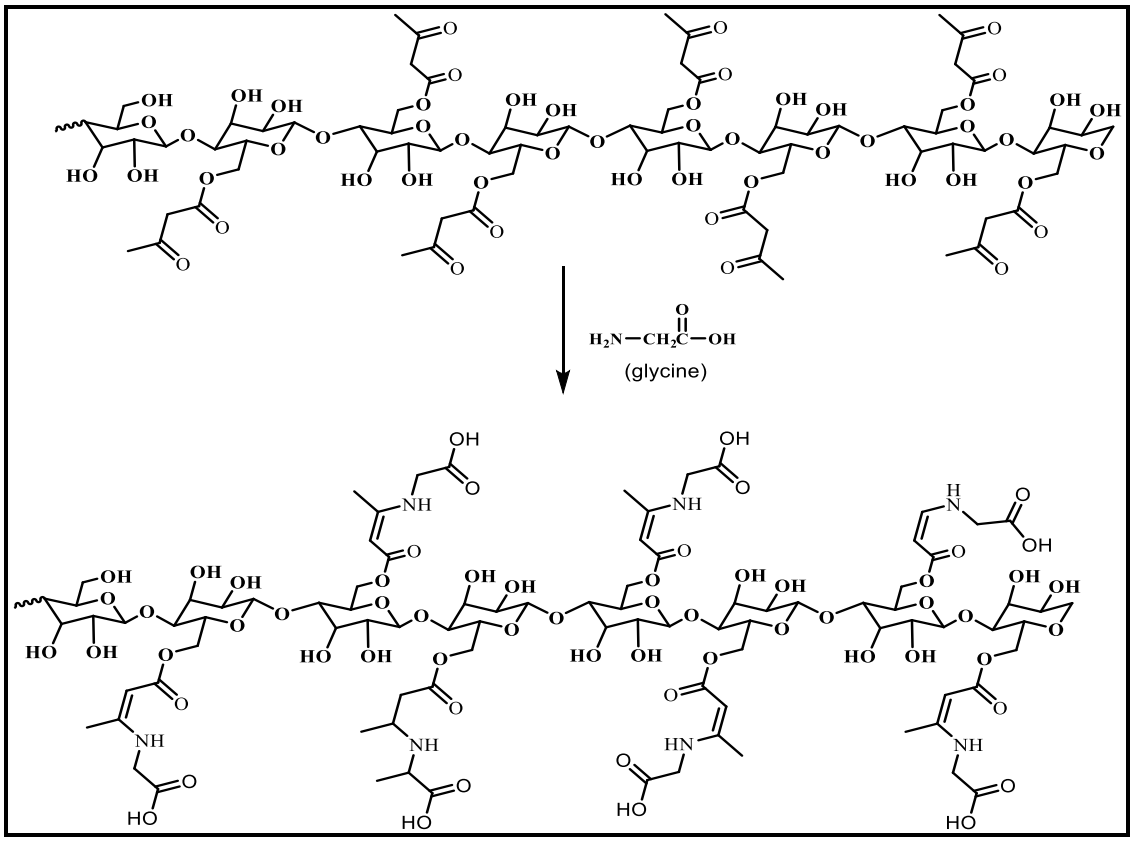

Fig (3.11): Preparation of cellulose β-aminoacetonate using glycine.

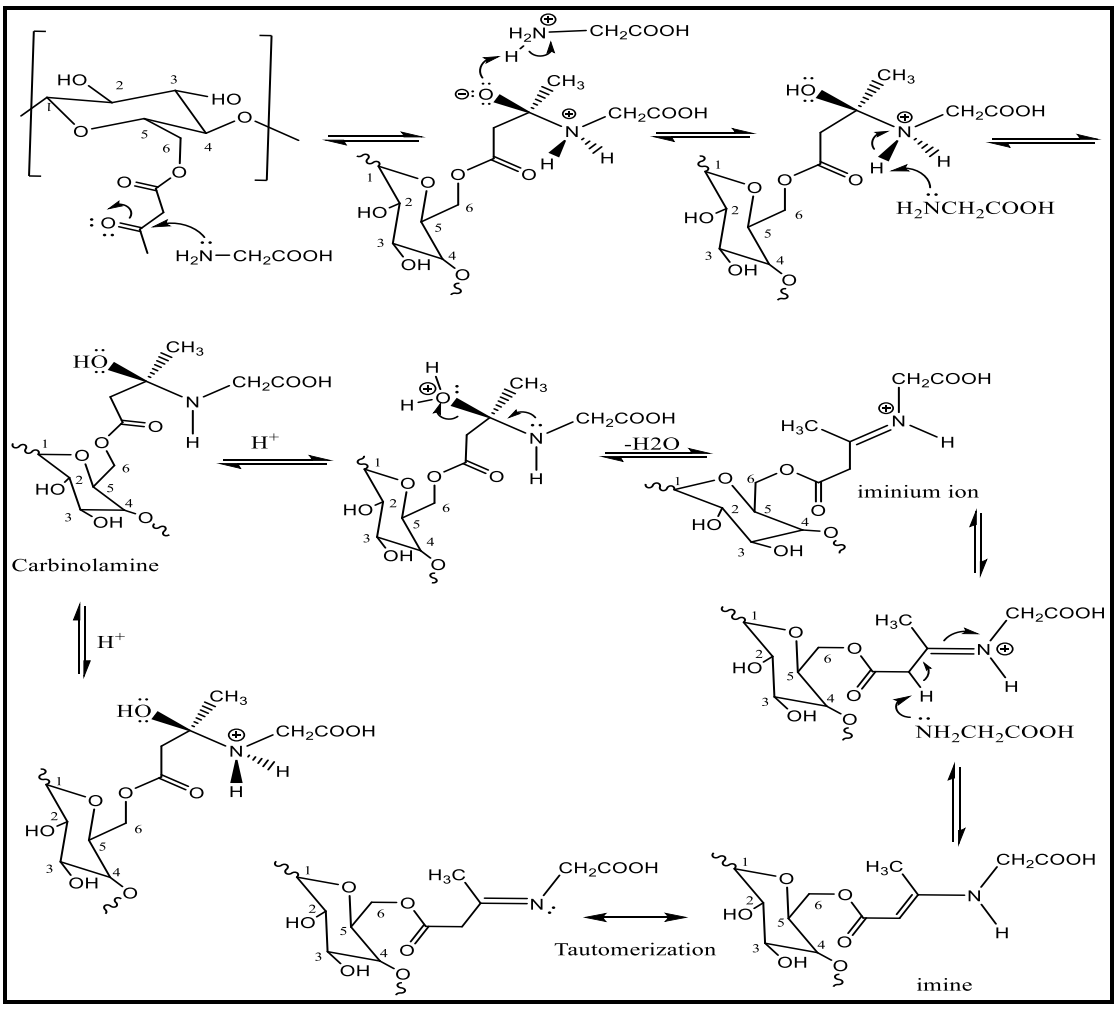

Fig (3.12): mechanism of synthesis of cellulose β-glycineacetonate

The adsorbents are expected to have a high affinity for various metals because the functional groups are considered multidentate chelating agents. as shown in fig 3.13. The produced polymers have several coordination sites for metal ions including amines, carbonyl, hydroxyl and aromatic functionalities. Amine and carbonyl are known to have a tendency to complex with metal ions due to their lone pair of electrons.

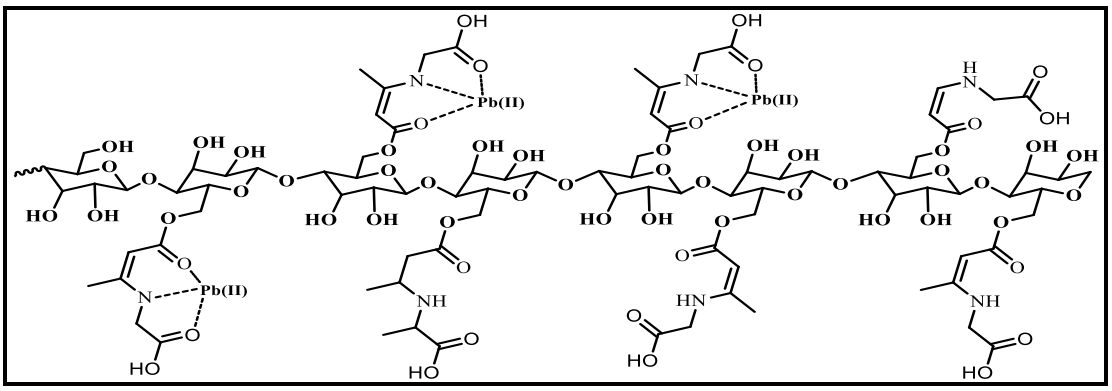

Fig (3.13): Cellulose aminoacetonate as a multidentate chelating agent (Shiff base)

3.3.1 FT-IR of cellulose β-glycineacetonate

The FT-IR spectrum of the Cell-β-GL is shown in Figure 3.14. The board strong peak at 1713 cm^{-1} that is composed of several peaks that overlapped together, which could be attributed to C=O of ester and carboxyl groups. The broad peak at about 3300 cm^{-1} is attributed to hydrogen bonded hydroxyl group (O-H of alcohol and carboxyl)) stretching. The presence of the 3452 cm^{-1} peak and disappear of the ketone domain at 1709 is an indication that the amine linkage is formed. The amine peak is not sharp which could be due to overlap with hydroxyl group peak. The IR spectrum shows three bands at about 1152, 1050 and 1030 cm^{-1} for C-O-C of ester, pyranose ring skeletal and to β-glycosidic linkage vibration respectively. The adsorption peak at 2963 cm^{-1} actually is corresponding to symmetric and asymmetric stretching vibration of the C-H bond.

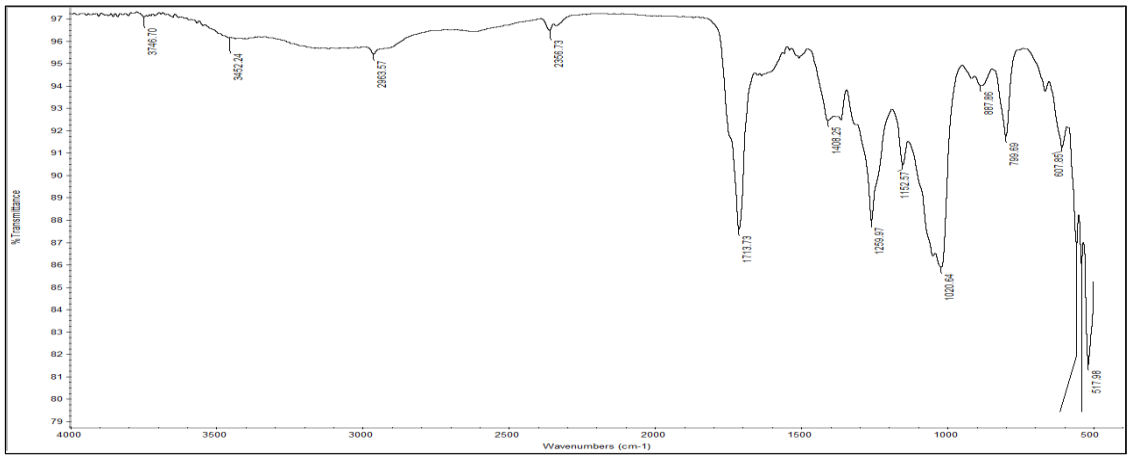

Fig (3.14): FT-IR spectrum for Cell-β-GL.

3.3.2 TGA analysis and thermal stability of Cell-β-GL

The thermal analysis was performed under air with a heating rate of 20 ºC per min during the analysis. The results of TGA analysis of Cell-β-GL is shown in figure 3.15.

The results show a big drop in the mass started at about 180 ^{o}C which could be attributed to the loss of the glycine acetonate side group. Complete decomposition of the of the polymer stated at about 470 ^{o}C. Again, the polymer is thermally stable considering the main purpose of making it which is wastewater purification.

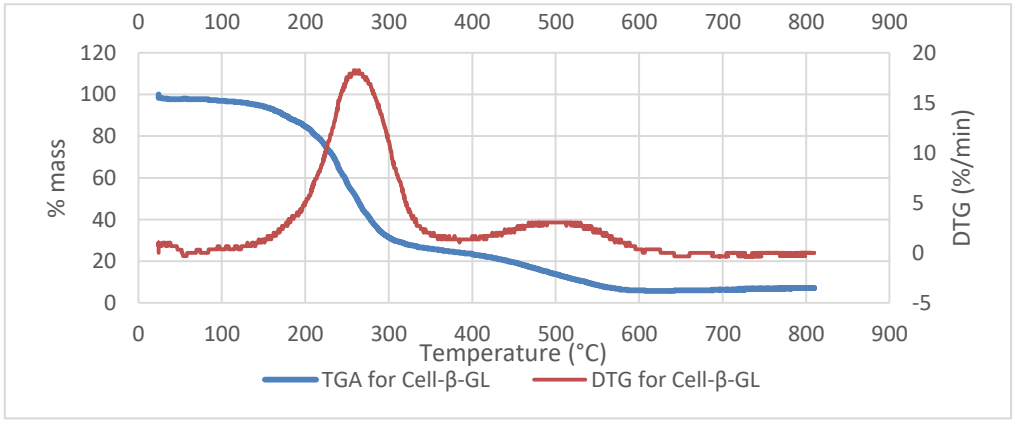

Fig (3.15): TGA and DTG analysis for Cell-β-GL polymer

3.4 Toxic Metal ions extraction

This research aims to use the prepared novel polymers shown above to extract heavy metal ions from wastewater, and to determine their adsorption efficiencies. The extraction was carried out using a batch adsorption process, in this process a known amount of three polymers (Cell-AA, Cell-β-AN, Cell-β-GL) was suspended in an aqueous solution of metal ions, then filtered and analyzed to determine the concentration of remaining ions in filtrate using atomic adsorption spectroscopy. Next the percentage of removal was determined for each uptake using equation 1.

$$R\,(\%) = \frac{C_0 - C_e}{C_0}\,100 \qquad (1)$$

The effect of several variables such as adsorbent dosage, metal ion concentration, extraction time, temperature and pH were investigated to determine best conditions for the highest adsorption efficiency. The adsorption study was performed on lead ions.

The adsorbent efficiency (percent removal of lead ions) and the adsorption capacities (the amount of metal ion adsorbed by unit mass of polymers) was determined according to Equations. 1 and 2 respectively.

$$Q_e = \frac{C_0 - C_e}{m} V \qquad (2)$$

C_0 and C_e are the initial and equilibrium concentration (ppm) of metal ion in solution respectively, Q_e (ppm) is the equilibrium adsorption capacity of the adsorbent (mg/g), m is the weight of the adsorbent (g), and V is the volume of the solution (L).

3.4.1 Optimum adsorption conditions

3.4.1.1 Adsorbent dosage

The experimental results of the removal of Pb(II) ions with respect to the dose of adsorbents Cell-AA, Cell-β-AN and Cell-β-GL are shown in Figure 3.5.1 over a range of 5.0 mg to 50.0 mg. The dosage that resulted in the lowest residual concentration of metal ion was chosen as an optimum dosage. This was achieved by performing the experiment on 10 ml of each Pb^{2+} with a concentration of 10.0 ppm, pH value of 4.3 for 30 min and at room temperature. From Figure 3.16, its clear that the amount of metal extracted increased by increasing the polymer dosage. Metal ion removal reached about 40.9, 35.1 and 60.5% for Pb^{+2} at 40.0 mg of dose of Cell-AA, Cell-β-AN and Cell-β-GL polymers, respectively, at dose higher than 40.0 mg it tends to stay almost constant. This could be because the adsorption process is structured by two mechanisms, diffusion and surface complexation. As the polymer dosage increases, the number of available vacant binding sites increase, and the unsaturated adsorption site increases so the removal efficiency increases. When all coordination site on the surface become saturated, the diffusion process starts, which is controlled by osmosis. When the concentration of metal ion adsorbed at polymer surface equal to the free ion in solution the adsorption stops [17]. The optimum dosage that was chosen to complete the examination of the effect of the other variables was 50.0 mg of each polymer because it produced the highest removal of lead ions.

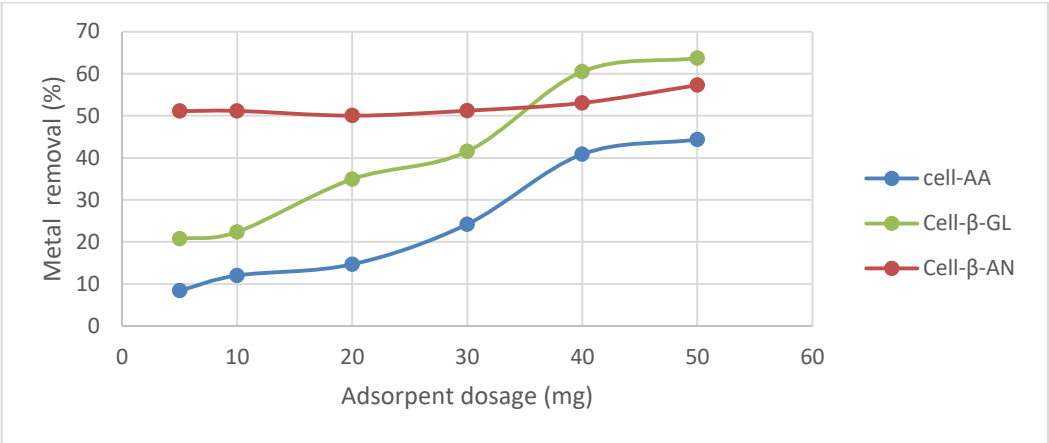

Fig (3.16): The effect of the three polymers dose on the removal efficiency

3.4.1.2 Optimum contact time

Adsorption of the lead metal ions by cellulose-based polymers as a function of time was evaluated under conditions of pH 4.3, initial ion concentration 10 ppm, volume of adsorbate 10 ml, adsorption temperature 25 ^{o}C and adsorbent dose 50.0 mg. The contact time that obtained the lowest residual concentration of metal ion was chosen as an optimum contact time. Results are shown in Figure 3.17, as shown in the figure, the adsorbed metal ions increased rapidly for the first 30 min for Cell-β-AN polymer and for 120 min for Cell-AA and Cell-β-GL polymer due to the availability of the binding sites on the outer surface of the adsorbent. Followed by almost stability in the adsorption rate for the remaining time. Cell-β-AN polymer reached to the equilibrium after 30 min, while Cell-AA and Cell-β-GL polymer reached equilibrium at about 120 min, so at these periods almost all coordination sites are occupied [81]. A contact time of 30 min was chosen as the optimum contact time for the three polymers. Based on that, we note that the Cell-β-AN polymer is better than Cell-AA and Cell-β-GL

because it removes a higher percentage of Lead(II) ions with less contact time.

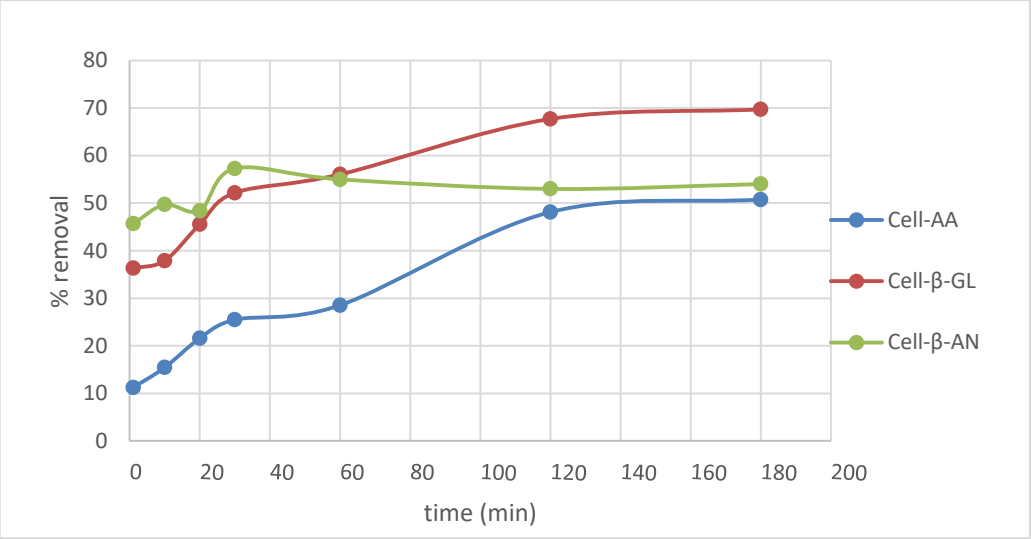

Fig (3.17): The effect of contact time on the removal efficiency of the three polymers

3.4.1.3 Optimum temperature

The effect of temperature on the removal of Pb(II) ions by the three polymers was studied under conditions of pH 4.3, volume of adsorbate 10.0 ml, initial metal ion concentration 10.0 ppm, adsorption time 30 min and adsorbent dose of 50.0 mg. The temperature that provided the lowest residual concentration of metal ion was chosen as an optimum temperature. Results are shown in Figure 3.18, as shown in the figure, the adsorption of lead ions using the three polymers increases with increasing temperature until a maximum at 30 ^{o}C is reached. After that, the percentage of removal decreases as the temperature is raised. The 30 ^{o}C was chosen as the optimum temperature for the three polymers. The percentage removed at the optimum temperature value are 44.353% for Cell-AA, 57.292% for

Cell-β-AN and 63.711% for Cell-β-GL. At lower temperature, the complexing capacities between lead ions and the polymers were enhanced, thus the bonding of Pb(II) with the adsorbent surface was increased. This result is an indication that the adsorption process is spontaneous at room temperature. At higher temperature value, over 30 ^{o}C, the percentage of metal removal decreased. The adsorption process is exothermic, as temperature increase, the kinetic energy of the adsorbed particle on the adsorbent surface increase, which leads to an increase in the possibility of separating them from the adsorbent surface and therefore the bonding ability between Pb(II) ions and the adsorbent surface become lower.

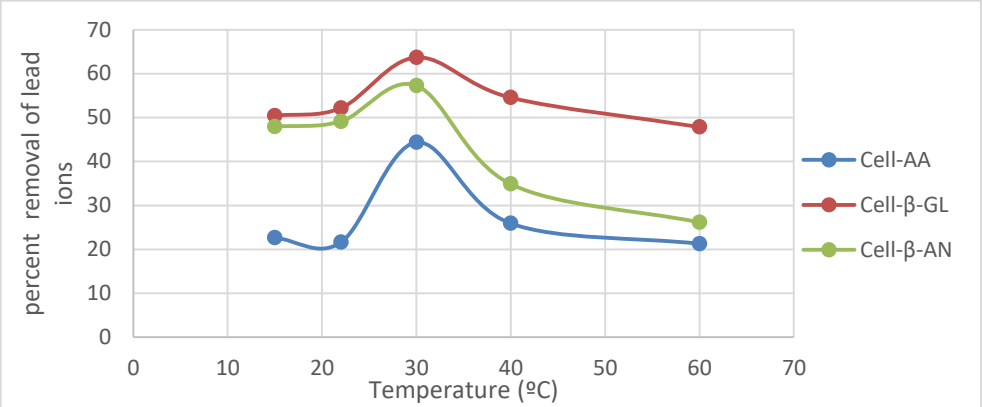

Fig (3.18): The effect of temperature on the removal efficiency of the three polymers

3.4.1.4 Initial lead(II) solution concentration

The effect of the initial lead ions concentration on adsorption efficiency for the three polymers was evaluated under the following adsorption conditions: adsorption time 30 min, adsorbent dose 50.0 mg, temperature 30 ^{o}C, volume of adsorbate 10 ml and pH 4.3. As shown in Fig 3.19 the maximum removal was at 10 ppm initial concentration of Pb(II), at this

concentration the % removal of ions reached 44.4% for cell-AA, 57.29% for Cell-β-AN and 63.7 % for Cell-β-GL. At concentration higher than 10 ppm the rate of adsorption decreases with increasing the concentration of lead ions in the solution. The results show that, at low concertation of lead ions, there are a sufficient binding site and the adsorption process is controlled by ion diffusion [81]. While at higher concentration, the availability of the binding sites decreases until the binding site are almost saturated, and the adsorption process is controlled by the adsorbent dosage. for this reason, at a concentration higher than 10 ppm, the lead removal rate decreased.

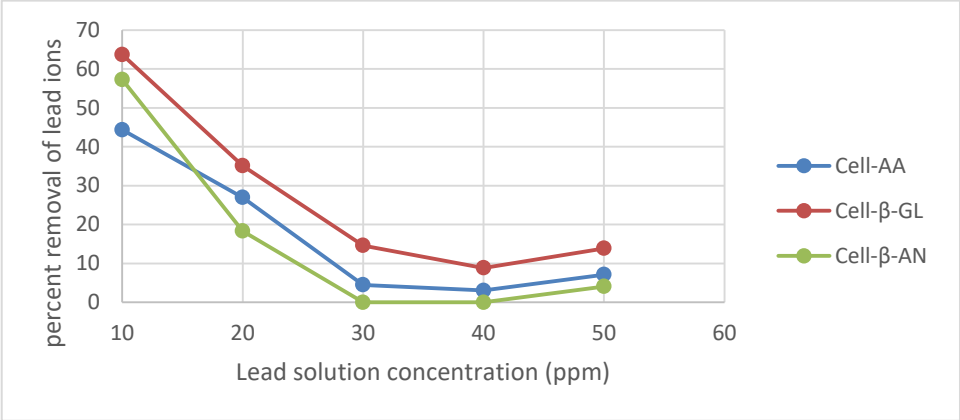

Fig (3.19): The effect of lead solution concentration on the removal efficiency for the three polymers

3.4.1.5 Optimum pH

The effect of the pH value on adsorption efficiency for the three polymers was evaluated under the following experimental conditions: adsorption time 30 min, adsorbent dose 50.0 mg, temperature 30 ºC, initial ion concentration 10 ppm and volume of adsorbate 10 ml. The pH that provided the lowest residual concentration of metal ion was chosen as an

optimum pH. The effect of the pH on the removal of Pb(II) ion by three polymers is shown in fig 3.20. The pH value is the most important factor that controlling the adsorption of metal ions from aqueous solution, because its influence on the polar polymers. At low pH value (lower than 3.0) the amine presence in ammonium form ($-NR_2H_2^+$), also the carboxyl and hydroxyl groups are in protonated form (COOH and OH), so the adsorption efficiency was the low. While at higher pH than 4.5, the N and O lone pair of electrons in amine, carbonyl and hydroxyl groups start to become available. Since at a pH higher than 4.5, the amines, carbonyl and hydroxyl groups start to shift to the Lewis base form, the protons become partially bonded to O and N, the electrostatic repulsion between proton and metal ion decrease, causing the hydroxyl, carbonyl and amine behave as a stronger chelating agent. The highest efficiency was observed at pH 9. At pH value higher than 9, the adsorption efficiency started to decline, this decreasing is due to formation of soluble metal oxide complex which reduced the adsorption efficiency of Pb^{+2} from the aqueous solution. So, the optimum pH value at about 9.

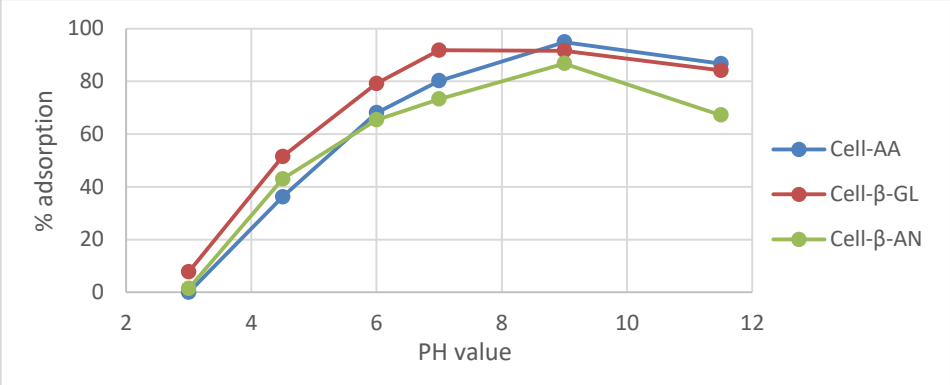

Fig (3.20): The effect of pH on the removal efficiency of the three polymers

3.5 Wastewater purification from metals

The efficiency of the modified cellulose polymers (Cell-AA, Cell-β-AN and Cell-β-GL) and their ability to adsorb toxic metal ions present in real wastewater sample generated from human activities at homes, agriculture, or factories were tested.

Samples of sewage water were taken from Beit Dajan wastewater treatment plant in Palestine. This wastewater is classified as grade D. This grading regards to the water when it leaves the treatment plant. Grade D means water has unsatisfactory level of risk, and treatment is not adequate. Grading was calculated using complex algorithm involving multiple tables. Each grade can be attained by a variety of factor combinations such as water's origin, characteristics, degree of treatment and compliance with standards. Three samples of this water were prepared to be treated with the prepared polymers. The concentrations of the metal ions in each of the sewage samples prior and after using the polymers are summarized in table (3.1, 3.2 and 3.3). Metal ions concentrations were measured using ICP-MS. Excellent efficiency was achieved against some metal ions present in the wastewater samples.

Table (3.1): Results of the center of analyzes for the Concentration of toxic metals using Cell-AA polymer.

Metal Ions	Conc. Before (ppm)	Conc. After (ppm)	Percentage Removals (%)
Al	12.936	2	84.539
Ba	34.307	1.8	94.753
B	97.531	1.9	98.052
Cr	27.844	2.9	89.585

Cu	3.773	1.8	52.293
Fe	205.490	2.7	98.686
Pb	7.473	0.9	87.957
Mn	19.822	2.5	87.388
Ni	4.139	0.6	85.504
V	1.973	1.8	8.768
Zn	13.07	4.1	68.631

Table (3.2): Results of the center of analyzes for the Concentration of toxic metals using Cell-β-AN polymer

Metal Ions	Conc. Before (ppm)	Conc. After (ppm)	Percentage Removals (%)
Al	19.443	0.9	95.371
Ba	32.839	1.4	95.737
B	94.844	2.3	97.575
Cr	27.156	4	85.270
Cu	3.038	0.3	90.125
Fe	196.416	0.5	99.745
Pb	1.545	0.6	61.165
Mn	25.483	2.4	90.582
Ni	3.735	1.5	59.839
Zn	7.117	2.9	59.253

Table (3.3): Results of the center of analyzes for the Concentration of toxic metals using Cell-β-GL polymer.

Metal Ions	Conc. Before (ppm)	Conc. After (ppm)	Percentage Removals (%)
Al	18.534	3.3	82.195
Ba	24.727	1.9	92.316
B	97.404	2	97.947
Cr	24.325	3.7	84.789
Cu	3.676	2	45.593
Fe	166.782	3	98.201
Pb	11.402	1.2	89.476
Mn	17.873	2.7	84.893
Ni	4.342	1.2	72.363
Zn	12.707	4.5	64.587

3.6 Polymer adsorption cycle

The regeneration experiment was carried out to determine number of times the polymers can be used and the efficiency of the polymers. The experiment was repeated seven times using the same adsorbent and the result are shown in fig 3.21. The adsorption efficiency decreases as the number of regeneration cycles increases. In the seventh time, the Cell-AA, Cell-β-GL and Cell-β-AN polymers absorption of lead metals were 99% , 98.5% and 98.7% respectively.

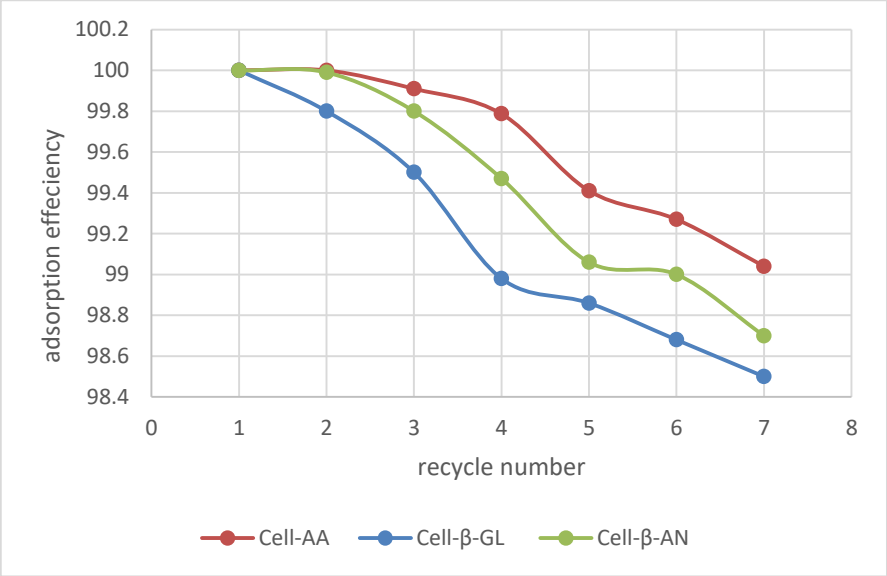

Fig (3.21): Regeneration and adsorption efficiency of the three polymers

3.7 Adsorption analysis

Langmuir (equation 3) and Freundlich isotherm (equation 5) models were applied to investigate the adsorption equilibrium between Pb^{2+} ion solution and the cellulose-based polymer [51]. Both models were used to assess the metal ion dispersion on the surface of the cellulose-based polymers once equilibrium is reached under constant temperature.

There are several isotherm models like Langmuir, Freundlich, etc. which can be applied at all temperatures. All of these models have equations that can be used, and the data will be fit into these equations. One of the factors that can lead to the type of isotherm model is the correlation coefficients, R^2 [51].

$$\frac{C_e}{Q_e} = \frac{1}{q_{max}} C_e + \frac{1}{q_{max} K_L} \qquad (3)$$

Where C_e represents the equilibrium concentration of the adsorbate (ppm), Qe is the amount of the adsorbate adsorbed per unit mass of cellulose based polymers at equilibrium (mg/g), q_{max} is the adsorption capacity equilibrium (mg/g), and K_L is usually, the Langmuir affinity constant (L/mg).

From Langmuir isotherm model Some authors define the R_L ratio as a dimensionless quantity indicating that sorption is favorable or not

$$R_L = \frac{1}{1 + K_L C_0} \qquad (4)$$

Where C_o is the initial adsorbate concentration. If the value of R_L is higher than 1, this indicates that the adsorption is unfavorable. However, when the R_L value is between 1 and 0, this indicates favorable adsorption, whereas when $R_L = 1$ indicates the presence of linear adsorption.

The other type of isotherm model is Freundlich isotherm is an empirical formula which used for low concentrations and can be presented as [51]:

$$\ln(q_e) = \ln k_F + \frac{1}{n} \ln Ce \qquad (5)$$

where K_F is the Freundlich constant that deal with adsorption capacity (mg/g) and n is the heterogeneity coefficient which leads to how favorable the adsorption process (g/L).

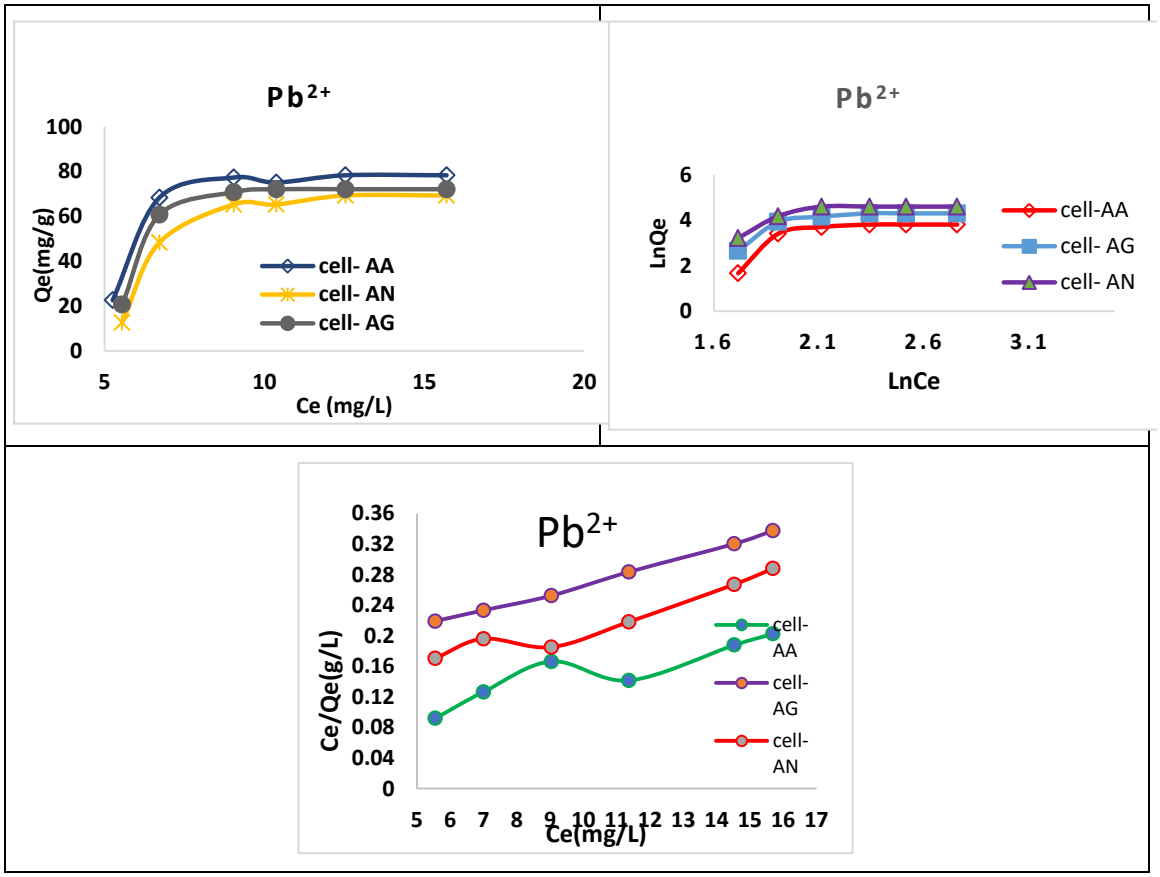

Fig (3.22): A) Langmuir adsorption model and B) Freundlich adsorption model of Pb^{2+} ions on cellulose-based polymers

Figure 3.22 summarizes all adjustment parameters. The correlation coefficients of the Freundlich isothermal model are lower than those of the Langmuir isothermal model (Table 3.4), reflecting that the adsorption of Pb^{2+} ions is in accordance with the Langmuir isothermal model, in which Pb^{2+} cations are distributed equally and homogeneously across the porous surfaces of the cellulose based polymers.

The separation factor R_L, which has been calculated for different quantities of adsorbent, ranges from $0< R_L<1$ (**Table 3.4**). This reflects the high degree of affinity of the cellulose based polymers for the studied metal ions.

Table (3.4): Langmuir and Freundlich parameters for the adsorption of Pb^{2+} ions by cellulose based polymers

		Pb^{2+}		
		Cell-AA	**Cell-β-GL**	**Cell-β-AN**
Langmuir isotherm	Q^0 (mg/g)	2.4587	2.1256	2.1254
	K_L (L/mg)	0.1524	0.1202	0.1965
	R_L			
	R^2	0.9625	0.8958	0.8548
Freundlich isotherm	1/n	1.2154	0.9587	1.2548
	K_F (L/mg)	16.325	23.3254	17.325
	R^2	0.8536	0.9621	0.93254

3.8 Adsorption kinetics of Pb^{2+} ions on cellulose based polymers

Presenting the experimental data through kinetics equations like the pseudo-first-order model, the pseudo-second-order model will describe the mechanism of adsorption of Pb^{2+} ions in aqueous solution. Such studies give information about the possible mechanism of adsorption of Pb^{2+} ions and different transition states on the final complex of Pb^{2+} ions and the adsorbent. From the reactions parameters like rate constants and adsorption capacity factors, one can have an idea about the adsorption dynamics and this will help the industry for other applications.

The adsorption experimental data of Pb^{2+} ions by the cellulose based polymers based of cellulose based polymers were analyzed using the most common kinetic models to understand the nature of the adsorption process.

The adsorption of metals by solid adsorbents such as cellulose based polymers was fattened to one of the most used kinetic models; pseudo-first order and pseudo-second order models, the equation can be written as the following. These kinetic models are shown in equations (7) and (8) [52].

$$\ln(q_e - q_t) = \ln q_e - K_1 t \qquad (7)$$

$$\frac{t}{q_t} = \frac{1}{K_{2q_e^2}} + \frac{t}{q_e} \qquad (8)$$

Weber and Morris developed an equation describing the intraparticle diffusion and can be written as the following equation [52].

$$Q_t = K_{id} t^{1/2} + Z \qquad (9)$$

where Q_t (mg g^{-1}) is adsorption capacity at any time t, k_{id} (mg/g $min^{1/2}$) is the intraparticle diffusion rate constant, and Z (mg/g) is a constant proportional to the thickness of the boundary layer.

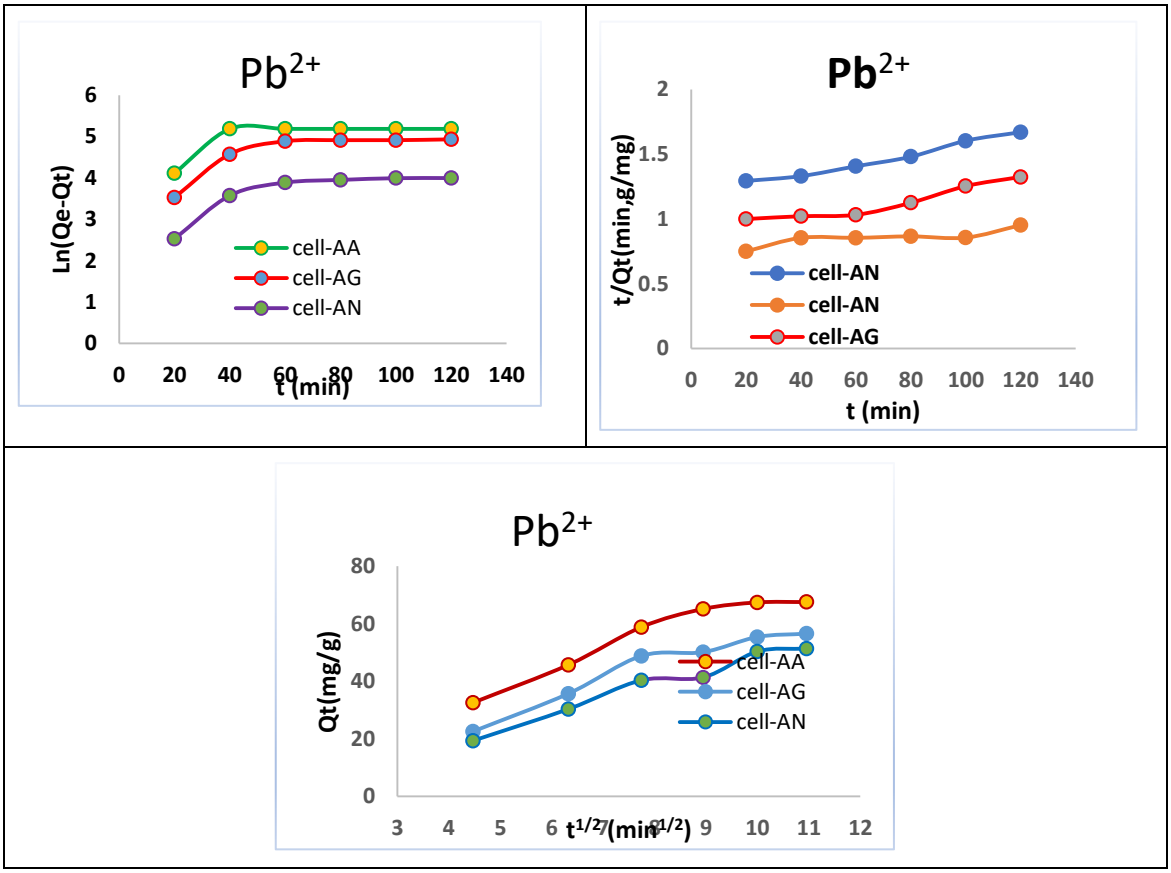

Fig 3.23. A) Pseudo first-order model for the adsorption of Pb2+, B) Pseudo-second order model for the adsorption of Pb2+ ions onto Cell-AA, Cell-β-AN, and Cell-β-GL. C) Intra-particle diffusion model for the adsorption of Pb2+ ions onto Cell-AA, Cell-β-AN, and Cell-β-GL at various concentrations.

Table 3.5 and Figure 3.23 summarize the values of all parameters of the above equations. The plots of Ln (qe-qt) versus t (Figure 3.23 A-D) provide the value of K1, whereas the values of K2 and the adsorption capacity qe were derived from the slope and intercept of the plot of t/Qt versus t (Figure 3.23 B-E) , while Kid and Z were deduced by tracing Qt vs t1/2 (Figure 3.23 C-F).

The experimental results show that the correlation coefficients (R2) for the pseudo-second order kinetics model (0.91 to 0.973) is greater than the pseudo-first order (0.891). A further indication was also provided by the

calculated qe values (2.675, 15.252, 20.856 mg/ g) which are similar to the experimental qe values (2.133, 13.91, 18.786 mg/ g) for the pseudo-second order model suggesting that the process of adsorption of Pb and Cu on the surfaces of the cellulose based polymers corresponds to the pseudo-second order (Table 3.5 and Figure 3.23B -E).

From (Figure 3.23C-F) (Qt vs. t1/2) Kid and Z were calculated and reported in Table 3.5. All graphs plotted in Figure 3.23 are straight line and didn't cross the origin, indicating the occurrence of more than one rate-limiting process.

Based on initial graphs linearity presented in Figure 3.23 B-E we can conclude that, at the outset of the adsorption process, the adsorption of Pb2+ on the cellulose based polymers takes place initially by an instantaneous adsorption step (on the external surface), which caused a chemical complexation between the metal ions and OH and further functionalities [53- 62]. The other steps were also linear, showing a progressive adsorption of Pb2+ ions and the step of limiting intraparticle diffusion rate.

The results presented in Table 3.5 reveal that the Z values reflect an expansion in the upper layer and a decrease in the outer mass transfer although the inner mass transfer potential was increasing. The energy of

activation of the adsorption process was computed at 298 and 323K according to Equation 9.

These findings are important for understanding how temperature influences adsorption performance of Pb2+ ions on the cellulose based polymers. The activation energy computed was nearly zero, suggesting a spontaneous adsorption process

Table (3.5): The pseudo-second-order model for adsorption of Pb^{2+} ions onto cell-AA, Cell-β-AN , and Cell-β-GL

	Cell-AA			**Cell-β-GL**				**Cell-β-GL**	
	K_2 (g/mg.min)	**Q_{cal}** (mg/g)	R^2	K_2 (g/mg.min)	Q_{cal} (mg/g)	R^2	K_2 (g/mg.min)	Q_{cal} (mg/g)	R^2
Pb^{2+}	0.3356	427.3254	0.9885	0.4325	548.3224	0.9750	0.465	632.2134	0.9887

Parameters explain the intra-particle diffusion of Pb^{2+} ions onto Cell-AA, Cell-β-AN, and Cell-β-GL.

	Cell-β-GL			**Cell-β-GL**			**Cell-β-GL**		
	K_{id}	**Z**	**R^2**	**K_{id}**	**Z**	**R^2**	**K_{id}**	**Z**	**R^2**
Pb^{2+}	0.1625	5.9021	0.9402	0.1503	5.8507	0.9514	0.1844	5.6977	0.9465

Thermodynamic parameters for the adsorption of Pb^{2+} ions onto Cell-AA, Cell-β-AN , and Cell-β-GL

	Pb^{2+}		
	ΔG° (KJ/mol)	**ΔH°** (KJ/mol)	**ΔS°** (J/K.mol)
Cell-β-GL	-17.2525	13.20211	74.92155
Cell-β-GL	-18.2314		
Cell-β-GL	-18.8021		
	K_{df}	R^2	
Cell-β-GL	0.093	0.9685	
Cell-β-GL	0.0849	0.9725	
Cell-β-GL			

3.9 Thermodynamics study

In this study, different parameters were calculated like the standard free energy, standard enthalpy, and standard entropy. The aim of this study is to understand spontaneity and to understand the nature of adsorption. The following equation was used [52]:

$K_c = C_{ads}/C_e$ (11) $\Delta G^0 = -RT\ln K_c$ (12) $\ln K_s = \frac{\Delta S}{R} - \frac{\Delta H}{RT}$ (13)

where K_c is an apparent constant of the thermodynamics; and C_{ads} and C_e are respectively the amount adsorbed at equilibrium (ppm) and concentration of metal ion in the solution (ppm), R is the universal gas constant (8.314J/mol K); T is the solution temperature [54]. The (ΔG^0) (J mol^{-1}) value was determined according to equation 12. The ln K_s *vs.* 1/T was mapped as illustrated in Figure 3.24, the slopes and crossings were utilized to determine various thermodynamics parameter as shown in Table 3.5.

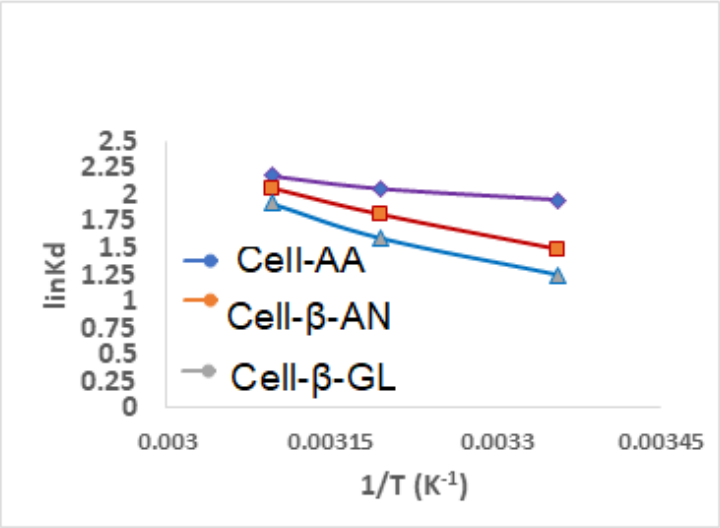

Fig (3.24): Adsorption thermodynamics of Pb^{2+} ions onto cell-AA, Cell-β-AN, and Cell-β-GL.

The value obtained for ΔS^0 and ΔH^0 are positive, whereas the entropy raised at the solid/solution interface induced as a result of the adsorption process. The findings further indicate that, all free energies for the cellulose based polymers were negative reflecting a spontaneous process of adsorption at various temperatures.

The metal removal mechanism by adsorption generally occurs at various stages. In the first step, metal ions migrate from most of the solution to the outer surface of the cellulose based polymers, then diffuse across the boundary-layer to the outer surface of the cellulose based polymers, followed by adsorption of metals ions at active sites on the cellulose based polymers surface, and lastly, intra-particle diffusion and adsorption of ions across the cellulose based polymers particles. Consequently, the sorption mechanism was investigated using the liquid film model and the intra-particle diffusion model.

The model of liquid film diffusion implies that the flow of adsorbate particles through a liquid film around the solid adsorbent is the longest phase in the adsorption process (i.e., the one that determines the kinetics of the velocity processes). The equation (10) describes the liquid film diffusion model.

$$\ln(1 - F) = k_{fd}\, t \qquad (10)$$

where F is the ratio ($F = q_t/q_e$) reached at the equilibrium, and k_{fd} (min^{-1}) is the film-diffusion coefficient. A linear plot of ln(1─F) versus t, at zero intercept, involve that the kinetics of the adsorption process is controlled by

the diffusion across the liquid film enclosing the cellulose based polymers. q_e is the adsorption capacity at equilibrium (mg. g^{-1}). Figure 3.25 highlighted that, using the liquid film diffusion model to the analytical results of Pb^{2+} adsorption by the cellulose based polymers from aqueous solution at various temperatures did not converge, didn't exhibit linear lines crossing the origin, and had very low correlation coefficients: 0.1876 and 0.1578 for Pb^{2+}, respectively. This suggests that diffusion of ions through the liquid film around the cellulose based polymers was not the step that determines the velocity. It should be noted that the liquid film diffusion model was used at the first few points during 10 min of adsorption, and the coefficients of regression were modestly enhanced to 0.9735 and 0.9873 for Pb^{2+}, respectively. These results suggest that the diffusion pattern of the liquid film is not the slowest step to determine the rate, but could affect the adsorption process, particularly at the commencement of adsorption, as indicated in Table 3.5.

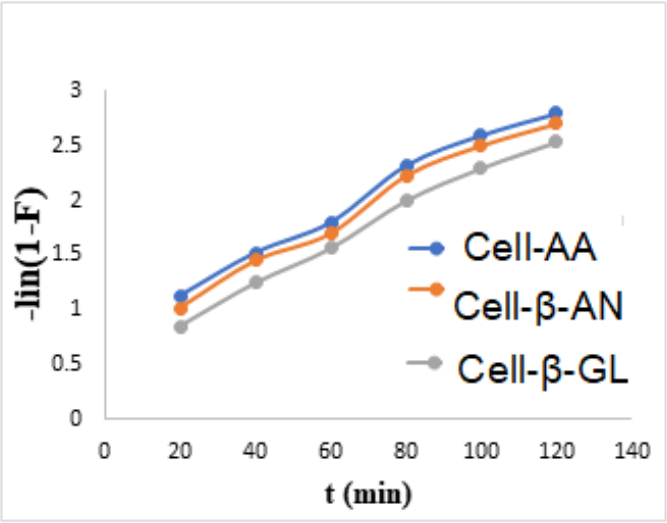

Fig (3.25): Liquid film diffusion model plots for the adsorption of Cell-AA, Cell-β-AN, and Cell-β-GL

Conclusions

In this work, the t-Butyl acetoacetate (t-BAA) underwent transesterification with cellulose to form cellulose acetoacetate in the presence of DMAc/LiCl solvent. A Cell-β-AN and Cell-β-GL polymers was prepared by reacting known amounts of cellulose acetoacetate with aniline and glycine, respectively in presence of HOAc as a catalyst. The structure of the three prepared polymers were identified by FT-IR, there thermal stability was also evaluated, all showed stability at a temperature as high as 200 ^{o}C. The meat adsorption efficiency of the three polymers for metal ions were evaluated. The cellulose fiber used in this work was extracted from olive industry solid waste by a process developed at our laboratories. Optimum adsorption conditions such as time, temperature, adsorption dosage, metal ion initial concertation, and pH values have been determined to achieve the highest adsorption efficiency for the polymers. The polymers showed an excellent efficiency toward Pd(II) metals due to the abundance of vacant sites for bonding of metallic ions on the surfaces of the polymers. The highest absorbency was observed at pH of approximately 9.0 at 30 ^{o}C. The three polymers showed almost equal efficiency for the metal ions Pb(II).

A sample was collected from a real mixture of wastewater that contained approximately 20 metal ions and treated with the prepared polymers. The removal efficiency of toxic metal ions present in the wastewater sample was high and remarkable. The three polymers showed a high percentage of lead adsorption after being recycled for seven times.

Recommendations

a. These polymers can be screened in water treatment for organic pollutants.
b. These polymers can be investigated in various applications in different areas of drug administration and the pharmaceutical industry.
c. These polymers can be screened in water treatment for other toxic heavy metal.
d. A film can be produced from the cross-linked of the three polymers and the effect of this cross-linked can be examined.

References

[1] Manahan, S. (2017). Environmental chemistry, 7th edition. CRC press.

[2] O'Neil, P. (2017). Environmental chemistry. Routledge.

[3] Chaudhry, F. N., & Malik, M. F. (2017). Factors affecting water pollution: a review. *J Ecosyst Ecography*, *7*(225), 1-3.

[4] Arif, A., Malik, M. F., Liaqat, S., Aslam, A., Mumtaz, K., Afzal, A., ... & Javed, R. (2020). 3. Water pollution and industries. *Pure and Applied Biology (PAB)*, *9*(4), 2214-2224.

[5] Colin Baird (2012) Environmental chemistry, 5th edition.

[6] Connor, R. (2015). The United Nations world water development report 2015: water for a sustainable world (Vol. 1). UNESCO publishing.

[7] Goel, P. K. (2006). *Water pollution: causes, effects and control*. New Age International.

[8] Shawai, S. A. A., Muktar, H. I., Bataiya, A. G., Abdullahi, I. I., Shamsuddin, I. M., Yahaya, A. S., & Suleiman, M. (2017). A review on heavy metals contamination in water and soil: effects, sources and phytoremediation techniques. *International Journal of Mineral Processing and Extractive Metallurgy*, *2*(2), 21-27.

[9] Bharathy, N. (2018). Water pollution and water quality standards for livestock.

[10] Obinna, I. B., & Ebere, E. C. (2019). A review: Water pollution by heavy metal and organic pollutants: Brief review of sources, effects and

progress on remediation with aquatic plants. Analytical Methods in Environmental Chemistry Journal, 2(03), 5-38.

[11] Junior, A. C. G., Schwantes, D., Junior, E. C., Zimmermann, J., & Coelho, G. F. (2021). Adsorption of Cd (II), Pb (II) and Cr (III) on chemically modified Euterpe Oleracea biomass for the remediation of water pollution. *Acta Scientiarum. Technology*, *43*, e50263-e50263.

[12] da Paz Schiller, A., Ferronato, M. C., Schwantes, D., Gonçalves Jr, A. C., Barilli, D. J., & Manfrin, J. (2019). Influence of hydrological flows from tropical watersheds on the dynamics of Cu and Zn in sediments. *Environmental monitoring and assessment*, *191*(2), 86.

[13] Slob, W. (1999). Thresholds in toxicology and risk assessment. *International Journal of Toxicology*, *18*(4), 259-268.

[14] Masindi, V., & Muedi, K. L. (2018). Environmental Contamination by Heavy Metals, Heavy Metals, Hosam El-Din M. Saleh and Refaat F. Aglan, IntechOpen.

[15] Ahamed, M. I., & Lichtfouse, E. (Eds.). (2020). *Water Pollution and Remediation: Heavy Metals*. Springer.

[16] Sud, D., Mahajan, G., & Kaur, M. P. (2008). Agricultural waste material as potential adsorbent for sequestering heavy metal ions from aqueous solutions–A review. *Bioresource technology*, *99*(14), 6017-6027.

[17] Abdel-Ghani, N. T., Hefny, M., & El-Chaghaby, G. A. (2007). Removal of

lead from aqueous solution using low cost abundantly available adsorbent. *International Journal of Environmental Science & Technology*, *4*(1), 67-73.

[18] Mohammed, A. S., Kapri, A., & Goel, R. (2011). Heavy metal pollution: source, impact, and remedies. In *Biomanagement of metal-contaminated soils* (pp. 1-28). Springer, Dordrecht.

[19] P.K. Gautam, R.K. Gautam, M.C. Chattopadhyaya, S. Banerjee,

M.C. Chattopadhyaya, J.D. Pandey, Heavy metals in the environment: fate,

transport, toxicity and remediation technologies Thermodynamic profiling of

pollutants View project Materials for Solid oxide fuel cells View project Heavy

Metals in the Environment: Fate, Transport, Toxicity And Rem, 2016.

[20] Briffa, J., Sinagra, E., & Blundell, R. (2020). Heavy metal pollution in the environment and their toxicological effects on humans. *Heliyon*, *6*(9), e04691.

[21] Okereafor, U., Makhatha, M., Mekuto, L., Uche-Okereafor, N., Sebola, T., & Mavumengwana, V. (2020). Toxic metal implications on agricultural soils, plants, animals, aquatic life and human

health. *International journal of environmental research and public health*, *17*(7), 2204.

[22] K.chojnacke & M.Mikulewicz. (2014). Bioaccumulation. Encyclopedia of toxicology, 3rd edition , 450-460.

[23] Joseph, L., Jun, B. M., Flora, J. R., Park, C. M., & Yoon, Y. (2019). Removal of heavy metals from water sources in the developing world using low-cost materials: A review. *Chemosphere*, *229*, 142-159.

[24] Engwa, G. A., Ferdinand, P. U., Nwalo, F. N., & Unachukwu, M. N. (2019). Mechanism and health effects of heavy metal toxicity in humans. Poisoning in the modern world-new tricks for an old dog, 10.

[25] Ali, H & ,.Khan, E. (2019). Bioaccumulation of Cr, Ni, Cd and Pb in the economically important freshwater fish Schizothorax plagiostomus from three rivers of Malakand Division, Pakistan: risk assessment for human health. Bulletin of environmental contamination and toxicology, 102(1), 77-83.

[26] Lalor, G. C. (2008). Review of cadmium transfers from soil to humans and its health effects in the Jamaican environment. Science of the total environment, 400(1-3), 162-172.

[27] Duruibe, J. O., Ogwuegbu, M. O. C., & Egwurugwu, J. N. (2007). Heavy metal pollution and human biotoxic effects. *International Journal of physical sciences*, *2*(5), 112-118.

[28] Singh, J., & Kalamdhad, A. S. (2011). Effects of heavy metals on soil, plants, human health and aquatic life. *International journal of Research in Chemistry and Environment*, *1*(2), 15-21.

[29] Genchi, G., Sinicropi, M. S., Carocci, A., Lauria, G., & Catalano, A. (2017). Mercury exposure and heart diseases. *International journal of environmental research and public health*, *14*(1), 74

[30] Mazumder, D. G. (2008). Chronic arsenic toxicity & human health. *Indian J Med Res*, *128*(4), 436-447.

[31] Ab Latif Wani, A. A., & Usmani, J. A. (2015). Lead toxicity: a review. *Interdisciplinary toxicology*, *8*(2), 55.

[32] Abadin, H., Ashizawa, A., Llados, F., & Stevens, Y. W. (2007). Toxicological profile for lead.

[33] Vigil, K. M. (2003). Clean water. As Introduction to Water Quality and Water Pollution Control.

[34] Organization WH. Guidelines for drinking-water quality: First addendum to volume 1, Recommendations: World Health Organization; 2006.

[35] Faust SD, Aly OM. Chemistry of water treatment: CRC Press; 1998.

[36] Milieu Ltd, W. (2014). RPA (2010) Environmental, economic and social impacts of the use of sewage sludge on land. 266. *URI: http://ec. europa. eu/environment/waste/sludge/pdf/part_iii_report. pdf. Cited*, *9*(7).

[37] Peng, H., & Guo, J. (2020). Removal of chromium from wastewater by membrane filtration, chemical precipitation, ion exchange, adsorption electrocoagulation, electrochemical reduction, electrodialysis, electrodeionization, photocatalysis and nanotechnology: a review. *Environmental Chemistry Letters*, 1-14.

[38] Taseidifar, M., Makavipour, F., Pashley, R. M., & Rahman, A. M. (2017). Removal of heavy metal ions from water using ion flotation. *Environmental Technology & Innovation*, *8*, 182-190.

[39] Silwamba, M., Ito, M., Hiroyoshi, N., Tabelin, C. B., Hashizume, R., Fukushima, T., ... & Ishizuka, M. (2020). Recovery of lead and zinc from zinc plant leach residues by concurrent dissolution-cementation using zero-valent aluminum in chloride medium. *Metals*, *10*(4), 531.

[40] Mcdonald, C. W., & Bajwa, R. S. (1977). Removal of toxic metal ions from metal-finishing wastewater by solvent extraction. *Separation Science*, *12*(4), 435-445.

[41] Bashir, A., Malik, L. A., Ahad, S., Manzoor, T., Bhat, M. A., Dar, G. N., & Pandith, A. H. (2019). Removal of heavy metal ions from aqueous system by ion-exchange and biosorption methods. *Environmental Chemistry Letters*, *17*(2), 729-754.

[42] Tsitonaki, A., Petri, B., Crimi, M., MosbÆK, H., Siegrist, R. L., & Bjerg, P. L. (2010). In situ chemical oxidation of contaminated soil and groundwater using persulfate: a review. *Critical Reviews in Environmental Science and Technology*, *40*(1), 55-91.

[43] Thaçi, B. S., & Gashi, S. T. (2019). Reverse osmosis removal of heavy metals from wastewater effluents using biowaste materials pretreatment. *Pol. J. Environ. Stud*, *28*(1), 337-341.

[44] Hashim, K. S., Shaw, A., AlKhaddar, R., Kot, P., & Al-Shamma'a, A. (2021). Water purification from metal ions in the presence of organic matter using electromagnetic radiation-assisted treatment. *Journal of Cleaner Production*, *280*, 124427.

[45] Alqadami, A. A., Naushad, M., ALOthman, Z. A., Alsuhybani, M., & Algamdi, M. (2020). Excellent adsorptive performance of a new nanocomposite for removal of toxic Pb (II) from aqueous environment: adsorption mechanism and modeling analysis. *Journal of hazardous materials*, *389*, 121896.

[46] Sen, T. K. (Ed.). (2017). *Air, gas, and water pollution control using industrial and agricultural solid wastes adsorbents*. CRC Press.

[47] Afroze, S., & Sen, T. K. (2018). A review on heavy metal ions and dye adsorption from water by agricultural solid waste adsorbents. *Water, Air, & Soil Pollution*, *229*(7), 1-50.

[48] Demirbas, A. (2008). Heavy metal adsorption onto agro-based waste materials: a review. Journal of hazardous materials, 157(2-3), 220-229.

[49] Qaiser, S., Saleemi, A. R., Umar, M. (2009). Biosorption of lead from aqueous solution by Ficus religiosa leaves: Batch and column study. *Journal of Hazardous Materials 166*, 998-1005.

[50] Ahamed, M. I., Lichtfouse, E & ,.Asiri, A. M. (Eds.). (2021). Green Adsorbents to Remove Metals, Dyes and Boron from Polluted Water. Springer.

[51] Anirudhan, T. S., & Sreekumari, S. S. (2011). Adsorptive removal of heavy metal ions from industrial effluents using activated carbon derived from waste coconut buttons. *Journal of Environmental Sciences*, *23*(12), 1989-1998.

[52] Uddin, M. K. (2017). A review on the adsorption of heavy metals by clay minerals, with special focus on the past decade. *Chemical Engineering Journal 308*, 438-462.

[53] Adeyemo, A. A.; Adeoye, I. O., Bello, O. S. (2017). Adsorption of dyes using different types of clay: a review. *Applied Water Sci*ence *7*, 543-568.

[54] Bo, S., Ren, W., Lei, C., Xie, Y., Cai, Y., Wang, S., Gao, J., Ni, Q., Yao, J. (2018). Flexible and porous cellulose aerogels/zeolitic imidazolate framework (ZIF-8) hybrids for adsorption removal of Cr(IV) from water. *Journal Solid State Chemistry 262*, 135-141.

[55] Chwastowski, J., Staroń, P., Kołoczek, H., Banach, M. (2017). Adsorption of hexavalent chromium from aqueous solutions using Canadian peat and coconut fiber. *Journal Molecular Liquids* 248, 981-989.

[56] Lin, J., Chen, X., Chen, C., Hu, J., Zhou, C., Cai, X., Wang, W., Zheng, C., Zhang, P., Cheng, J., (2018). Durably antibacterial and

bacterially anti-adhesive cotton fabrics coated by cationic fluorinated polymers. *ACS Applied Material Interface Science 10,* 6124-6136.

[57] Da Silva, J. S., Da Rosa, M. P., Beck, P. H., Peres, E. C., Dotto, G. L., Kessler, F., Grasel, F. S. (2018). Preparation of an alternative adsorbent from Acacia Mearnsii wastes through acetosolv method and its application for dye removal. *Journal Cleaner Production 180*, 386-394.

[58] Lin, J. X., Zhan, S. L., Fang, M. H., Qian, X. Q., Yang, H. (2008). Adsorption of basic dye from aqueous solution onto fly ash. *Journal of Environmental Management 87*, 193-200.

[59] Moa, J., Yanga, Q., Zhang, N., Zhang, W., Zheng, Y., Zhang, Z. (2018). Review on agro-industrial waste (AIW) derived adsorbents for water and wastewater treatment. *Journal of Environmental Management 227*, 395-405.

[60] Jodeh, S., Hamed, O., Melhem, A., Salghi, R., Jodeh, D., Azzaoui, K., Benmassaoud, Y., Murtada, K. (2018). Magnetic nanocellulose from olive industry solid waste for the effective removal of methylene blue from wastewater. *Environmental Science and Pollution Research 25*, 22060-22074.

[61] Chakraborty, R., Asthana, A., Singh, A. K., Jain, B., & Susan, A. B. H. (2020). Adsorption of heavy metal ions by various low-cost adsorbents: a review. International Journal of Environmental.

[62] Gupta, S., Babu, B. V. (2009). Utilization of waste product (tamarind seeds) for the removal of Cr(VI) from aqueous solutions: Equilibrium,

kinetics, and regeneration studies. *Journal of Environmental Management 90*, 3013-3022.

[63] Muhammad, R. R. Nor, A. Y., Mohammad, J. H., Norazowa, I., Faruq M., Sazlinda, K., Hamad A. A. (2018). Iminodiacetic acid modified kenaf fiber for waste water treatment. *International Journal of Biological Macromolecules 112*, 754-760.

[64] Karnitz, Jr O., Gurgel, L. V. A., de Melo, J. C. P. (2007). Adsorption of heavy metal ion from aqueous single metal solution by chemically modified sugarcane bagasse. *Bioresources & Technol*ogy *98*, 1291-1297.

[65] Doan, H. D., Lohi, A., Dang, V. B. H., Dang-Vu, T. (2008) Removal of Zn^{+2} and Ni^{+2} by adsorption in a fixed bed of wheat straw. *Process Safety Environmental Protection 86*, 259-267.

[66] Acar, F. N., Eren, Z. (2006). Removal of Cu(II) ions by activated poplar sawdust (Samsun clone) from aqueous solutions. *Journal Hazardous Materials 137*, 909-914.

[67] Vieira, M. G. A., de Almeida Neto, A. F., Da Silva, M. G. C., Carneiro, C. N., & Melo Filho, A. A. (2014). Adsorption of lead and copper ions from aqueous effluents on rice husk ash in a dynamic system. *Brazilian Journal of Chemical Engineering*, *31*, 519-529.

[68] Zelić, E., Vuković, Z., Halkijević, I. (2018). Application of nanotechnology in wastewater treatment. *GRAĐEVINAR 70*, 315-323.

[69] Wang, J., Liu, M., Duan, C., Sun, J., Xu, Y. (2019). Preparation

and characterization of cellulose-based adsorbent and its application in heavy metal ions removal. *Carbohydrate Polymers* 206, 837-843.

[70] Hugo Voisin, Lennart Bergstrom, Pangolin and Aji P. Mathew, 5 March (2017) Nano cellulose-Based materials for water purification: Review, 7(3). pii: E57. doi: 10.3390/nano7030057.

[71] Eyley, S., & Thielemans, W. (2014). Surface modification of cellulose nanocrystals. *Nanoscale*, *6*(14), 7764-7779.

[72] Schubert S, Schlufter K, Heinze T (2011). Configurations, structures, and morphologies of cellulose. In: Popa V (ed) polysaccharides in medicinal and pharmaceutical applications. iSmithers, Shrewsbury, pp 1-55.

[73] Blanco, A., Monte, M. C., Campano, C., Balea, A., Merayo, N & ,. Negro, C. (2018). Nanocellulose for industrial use: cellulose nanofibers (CNF), cellulose nanocrystals (CNC), and bacterial cellulose (BC). In Handbook of nanomaterials for industrial applications (pp. 74-126). Elsevier.

[74] Peng, B. L., Dhar, N., Liu, H. L., & Tam, K. C. (2011). Chemistry and applications of nanocrystalline cellulose and its derivatives: a nanotechnology perspective. The Canadian journal of chemical engineering, 89(5), 1191-1206.

[75] O'Connell, D. W., Birkinshaw, C., & O'Dwyer, T. F. (2008). Heavy metal adsorbents prepared from the modification of cellulose: A review. Bioresource technology, 99(15), 6709-6724.

[76] Granström, M. (2009). Cellulose derivatives: synthesis, properties and applications.

[77] Hamed, O., Fouad, Y., Hamed, E. M., Al-Hajj, N. (2012). Cellulose powder from olive industry solid waste. *BioResources*, *7*, 4190-4201.

[78] Hamed, O. A., Jodeh, S., Al-Hajj, N., Hamed, E. M., Abo-Obeid, A., & Fouad, Y. (2015). Cellulose acetate from biomass waste of olive industry. *Journal of wood science*, *61*(1), 45-52.

[79] Gupta, A. D., Pandey, S., Jaiswal, V. K., Bhadauria, V., & Singh, H. (2019). Simultaneous oxidation and esterification of cellulose for use in treatment of water containing Cu (II) ions. Carbohydrate polymers, 222, 114964.

[80] Zhou, Y., Hu, X., Zhang, M., Zhuo, X., & Niu, J. (2013). Preparation and characterization of modified cellulose for adsorption of Cd (II), Hg (II), and acid fuchsin from aqueous solutions. Industrial & Engineering Chemistry Research, 52(2), 876-884.

[81] Hamed, O., Lail, B. A., Deghles, A., Qasem, B., Azzaoui, K., Obied, A. A., ... & Jodeh, S. (2019). Synthesis of a cross-linked cellulose-based amine polymer and its application in wastewater purification. *Environmental Science and Pollution Research*, *26*(27), 28080-28091.

[82] Deghles, A., Hamed, O., Aza, M., Lail, B. A., Azzaoui, K., Obied, A. A., & Jodeh, S. (2019). Cellulose with Bidentate Chelating

Functionality: An Adsorbent for Metal Ions from Wastewater. BioResources, 14(3), 6247-6266.

[83] Kahl, T., Schröder, K. W., Lawrence, F. R., Marshall, W. J., Höke, H., & Jäckh, R. (2000). Aniline. Ullmann's Encyclopedia of Industrial Chemistry.

[84] Kearney, T. E., Manoguerra, A. S., & Dunford Jr, J. V. (1984). Chemically induced methemoglobinemia from aniline poisoning. Western Journal of Medicine, 140(2), 282.

[85] Amini, B., & Lowenkron, S. (2000). Aniline and its derivatives. Kirk-Othmer Encyclopedia of Chemical Technology.

[86] Rappoport, Z. (Ed.). (2007). The Chemistry of Anilines, Part 1 (Vol. 169). John Wiley & Sons, 294.

[87] National Center for Biotechnology Information (2021). PubChem Compound Summary for CID 750, Glycine. Retrieved August 31, 2021 from https://pubchem.ncbi.nlm.nih.gov/compound/Glycine

[88] Alves, A., Bassot, A., Bulteau, A. L., Pirola, L., & Morio, B. (2019). Glycine metabolism and its alterations in obesity and metabolic diseases. *Nutrients*, *11*(6), 1356.

[89] Razak, M. A., Begum, P. S., Viswanath, B., & Rajagopal, S. (2017). Multifarious beneficial effect of nonessential amino acid, glycine: a review. Oxidative medicine and cellular longevity, 2017.

[90] Wiley, L. (2007). Clavier. Kirk-Othmer Food and Feed Technology, 2 Volume Set.

[91] Robertson, G. R. (1927). The reaction of chloro-acetic acid with ammonia and the preparation of glycine. *Journal of the American Chemical Society*, *49*(11), 2889-2894.

[92] Sjöholm, E., Gustafsson, K., Eriksson, B., Brown, W., & Colmsjö, A. (2000). Aggregation of cellulose in lithium chloride/N, N-dimethylacetamide. *Carbohydrate Polymers*, *41*(2), 153-161.

[93] McCormick, C. L., Callais, P. A., & Hutchinson Jr, B. H. (1985). Solution studies of cellulose in lithium chloride and N, N – dimethylacetamide. *Macromolecules*, *18*(12), 2394-2401.

[94] Zhang, C., Liu, R., Xiang, J., Kang, H., Liu, Z., & Huang, Y. (2014). Dissolution mechanism of cellulose in N, N-dimethylacetamide/lithium chloride: revisiting through molecular interactions. The Journal of Physical Chemistry B, 118(31), 9507-9514.

[95] Fu, Y., Li, G., Wang, R., Zhang, F., & Qin, M. (2017). Effect of the molecular structure of acylating agents on the regioselectivity of cellulosic hydroxyl groups in ionic liquid. BioResources, 12(1), 992-1006.

[96] Rao, G. D., Acharya, B. N., & Kaushik, M. P. (2013). An efficient synthesis of β-ketoesters via transesterification and its application in Biginelli reaction under solvent-free, catalyst-free conditions. Tetrahedron Letters, 54(48), 6644-6647.

جامعة النجاح الوطنية

كليه الدراسات العليا

فيلم قائم على السليولوز مع قاعده شيف الوظيفيه: التحضير والتطبيق في امتزاز المعادن السامه من مياه الصرف الصحي

إعداد

نور رائد محمود نعيرات

إشراف

د. عثمان حامد

د. شحده جوده

قُدمت هذه الأطروحة استكمالا لمتطلبات الحصول على درجه الماجستير في الكيمياء من كليه الدراسات العليا في جامعه النجاح الوطنيه , نابلس – فلسطين.

2021

فيلم قائم على السليولوز مع قاعده شيف الوظيفيه: التحضير والتطبيق في امتزاز المعادن السامه من مياه الصرف الصحي

إعداد

نور رائد محمود نعيرات

إشراف

د. عثمان حامد

د. شحده جوده

الملخص

الهدف الرئيسي من هذا العمل هو استخدام مواد نفايات صناعة الزيتون كقاعدة أساسيه لصنع البوليمرات المناسبة لتنقية مياه الصرف الصحي من المعادن الثقيله السامه. تم استخدام السليلوز المستخرج من نفايات صناعة الزيتون الصلبة كمواد أوليه لإعداد ثلاثة مشتقات من السليلوز مع العديد من المواقع التنسيقيه والممتزات المفيده للايونات المعدنيه من مياه الصرف الصحي. تم استخدام السليلوز المستخرج من جفت الزيتون لتحضير اسيتو اسيتات السليلوز وامينو اسيتات السليولوز عن طريق إتباع الخطوات التالية:

أولاً: تم تذويب السليولوز في ثنائي ميثيل اسيتاميد/ كلوريد الليثيوم ثم تكثيفها مع ثلاثي بيوتيل اسيتو اسيتات، تحت جو خامل من النيتروجين على حراره 120 س لمده ساعتين ، بعد هذه المدة نتوقع تكون روابط ايسترية.

ثانياً: تفاعل اسيتو اسيتات السليولوز مع الانلين والجلايسين لانتاج مركبين من امينو اسيتات السليولوز لمده 6 ساعات، بعد هذه المدة نتوقع تكون روابط ببتيديه.

ثالثاً: تم تحديد هياكل البوليمرات باستخدام مطياف الاشعه تحت الحمراء.

رابعاً: تم فحص الثبات الحراري للبوليمرات باستخدام تقنيه التحليل الوزني الحراري؛ يجب ان يستقر عند درجه حراره حوالي 200 درجه مئويه.

خامساً: تم إجراء فحص فعالية المركبات الذي تم تحضيرها في امتصاص عنصر الرصاص من المياه الملوثة به .

سادساً: تمت دراسة أثر العديد من العوامل على فعالية إزالة عنصر الرصاص من المياه، وهذه العوامل هي: كمية البوليمر، والوقت الذي تعرضت له المياه الملوثة بالرصاص للبوليمر، ودرجة الحرارة، وتركيز محلول الرصاص ودرجة الحموضة، وذلك للتوصل للظروف المثالية التي تؤدي الى أقصى فعالية في إزالة عنصر الرصاص من المياه

سابعاً: بعد أن تم دراسة فعالية المركب وتحديد الظروف المعيارية لعمل المركب على تنقية المياه الملوثة تم استخدامه في تنقية مياه الصرف الصحي وقد اظهر نتائج ممتازة.

وكانت أعلى كفاءة من البوليمرات اسيتو اسيتات السليلوز وامينو اسيتات السليولوزالمصنوع من الجلايسين لأيون الرصاص 94.9٪ و 91.6٪، على التوالي، التي تم الحصول عليها بتركيز 10 جزء في المليون، 50 ملغ من كل البوليمر، في 30 درجة مئوية و 9 درجة الحموضة عند اهتزاز لمدة 120 دقيقة. بالنسبة للبوليمر امينو استات السليولوزالمصنوع من الانلين، كانت أعلى كفاءة تجاه أيون الرصاص 86.7٪ في نفس المعلمات السابقة تقريبا. بالإضافة إلى ذلك ، أظهرت البوليمرات القائمة على السليلوز كفاءة ممتازة تجاه معظم الأيونات المعدنية الموجودة في عينة الصرف الصحي.

وكانت أعلى كفاءة الامتزاز في درجة الحموضة من حوالي 9، 30 درجه سيليسيوس ومع 50 ملغرام من جرعة البوليمر. ويمكن أن يعزى ارتفاع كفاءة الامتزاز من البوليمرات القائمة على السليلوز إلى وجود مواقع التنسيق المختلفة التي تشمل الهيدروكسيل والأحماض الأمينية والكربونيل والحلقات الاروماتيه.

وعليه فان النتائج قد أظهرت قدرة عالية للبوليمر المحضر في امتصاص العناصر الملوثة السامة بنسب عالية وعليه يمكن استخدامه كمنقي ممتاز للمياه العادمة وإعادة استخدام المياه في الامور الزراعيه.